LBL-14406
Preprint c.2

Lawrence Berkeley Laboratory

UNIVERSITY OF CALIFORNIA

RECEIVED
LAWRENCE
BERKELEY LABORATORY

NOV 16 1982

LIBRARY AND
DOCUMENTS SECTION

Materials & Molecular Research Division

Submitted to the Journal of Catalysis

INFLUENCE OF ENSEMBLE SIZE ON CO CHEMISORPTION AND CATALYTIC n-HEXANE CONVERSION BY Au-Pt(111) BIMETALLIC SINGLE CRYSTAL SURFACES

J.W.A. Sachtler and G.A. Somorjai

June 1982

TWO-WEEK LOAN COPY

This is a Library Circulating Copy which may be borrowed for two weeks. For a personal retention copy, call Tech. Info. Division, Ext. 6782.

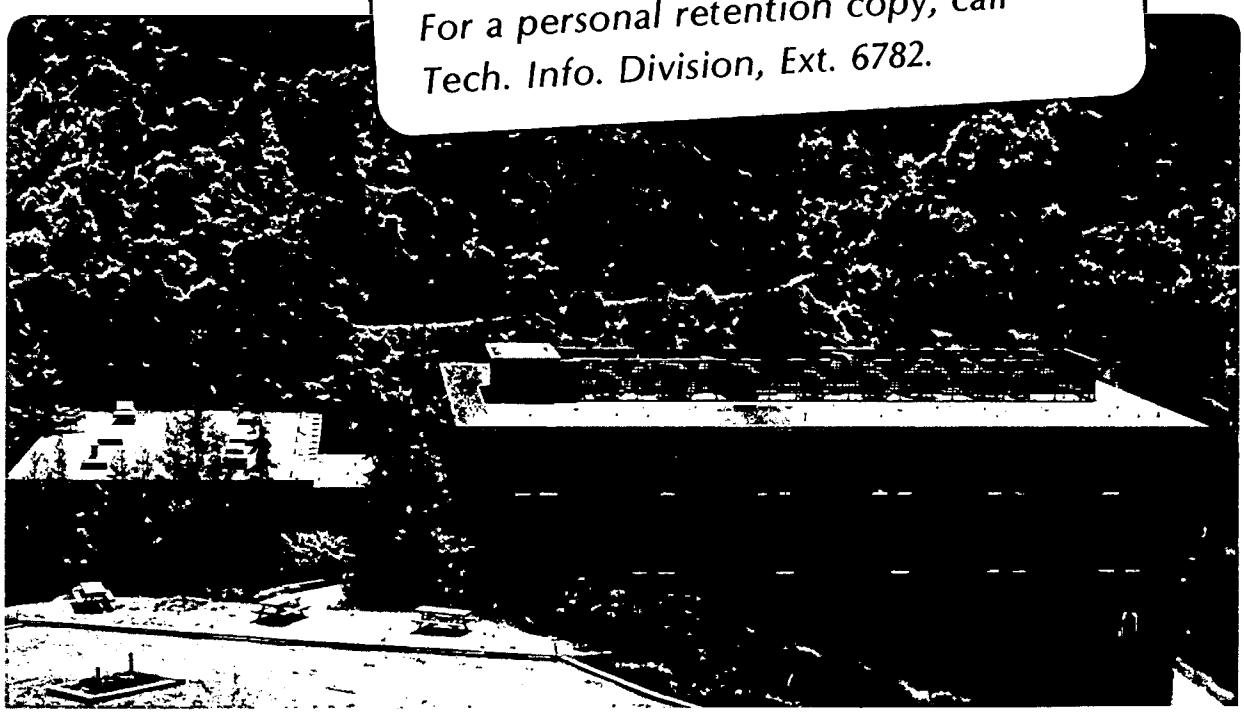

Prepared for the U.S. Department of Energy under Contract DE-AC03-76SF00098

LBL-14406 c.2

DISCLAIMER

This document was prepared as an account of work sponsored by the United States Government. While this document is believed to contain correct information, neither the United States Government nor any agency thereof, nor the Regents of the University of California, nor any of their employees, makes any warranty, express or implied, or assumes any legal responsibility for the accuracy, completeness, or usefulness of any information, apparatus, product, or process disclosed, or represents that its use would not infringe privately owned rights. Reference herein to any specific commercial product, process, or service by its trade name, trademark, manufacturer, or otherwise, does not necessarily constitute or imply its endorsement, recommendation, or favoring by the United States Government or any agency thereof, or the Regents of the University of California. The views and opinions of authors expressed herein do not necessarily state or reflect those of the United States Government or any agency thereof or the Regents of the University of California.

LBL-14406

INFLUENCE OF ENSEMBLE SIZE ON CO CHEMISORPTION AND CATALYTIC n-HEXANE CONVERSION BY Au-Pt(111) BIMETALLIC SINGLE CRYSTAL SURFACES

J.W.A. Sachtler and G.A. Somorjai

Materials and Molecular Research Division,

Lawrence Berkeley Laboratory

and Department of Chemistry, University of California

Berkeley, California 94720, USA

ABSTRACT

Epitaxial Au layers were prepared by vapor deposition of Au on a Pt(111) single crystal surface. Surface alloys were formed by heating the Pt(111) crystal that was covered with a Au multilayer. The surfaces were characterized with AES, LEED and TPD of CO. LEED showed that both gold overlayers and Pt-Au alloy surfaces were well ordered and had (1 x 1) surface structures. The temperature at the maximum of the TPD spectrum of CO was found to be sensitive to the distribution of Pt atoms in the surface. As a result, epitaxial surfaces were shown to have large Pt ensembles while much smaller ensembles were predominant on alloy surfaces. With TPD of CO it could also be demonstrated that the ligand effect of alloying is absent for CO adsorbed on these alloy surfaces. The differences in ensemble size were found to have profound effects on the skeletal reactions of n-hexane. This reaction was carried out *in situ* with 26.7 mbar (20 Torr) n-hexane in 267 mbar (200 Torr) hydrogen at 573 K, by utilizing a sample isolation cell.

Surface alloys were found to be more active than pure Pt(111). Large increases in the isomerization rate of n-hexane and simultaneous exponential decreases of hydrogenolysis and aromatization rates with gold coverage led to high selectivity for isomerization. Changes in the bonding of organic molecules must be responsible for this effect that are induced by structural alterations of the (111) orientation platinum crystal surface. Epitaxial gold layers decreased the activity of the Pt(111) surface in proportion to the gold coverage because of the reduction of the available platinum surface area, without substantial selectivity changes.

1. INTRODUCTION

As catalysts for hydrocarbon reactions, alloys of metals have received much attention.[1] Multicomponent systems may show improved activity, selectivity and stability. The two concepts that are used most widely to explain the altered catalytic properties are the "ensemble size" or "structural" and the "ligand" or "electronic" effects.[2]

Upon alloying of e.g. platinum with gold the concentrations of the various platinum surface sites, where the Pt atoms are surrounded by four, three or two in-plane nearest neighbors, are altered. As gold substitutes for Pt atoms the concentration of the higher coordination number, four-fold and three-fold sites that make up the large ensembles decreases more rapidly than the concentration of the low coordination number, (e.g., two-fold, single atom) small ensemble sites.

As a result, reactions that proceed through intermediates that are bound to many adjacent Pt atoms will be inhibited more strongly by alloying than reactions that require only small ensembles. The electronic effects are due to charge transfer from one of the alloy components to the other at a given surface site, which markedly alters the chemical bonding of reactants and reaction intermediates at that site leading to modified catalytic activity and selectivity. Although the two effects are not likely to be separable unambiguously, in the absence of large charge transfer from one of the alloy constituents to the other at a given surface site the structural effects may predominate. For the Pd-Ag system strong evidence for the predominance of the structural effect was obtained from an infrared spectroscopy investigation of chemisorbed CO.[3] It was found that upon alloying with Ag the the absorption band for CO that was bound to a multiplet of Pd atoms decreased more rapidly than the band for

CO adsorbed on top of a single Pd atom. TPD of hydrogen from Pt-Au alloy surfaces[4] did not show a shift of desorption peak temperatures which argues against a significant ligand effect for this system.

However, recent studies of the coadsorption of potassium and CO on platinum indicate that the large charge transfer from K to Pt increases the binding energy of the Pt-CO bond by 50 kJ/mole and also results in the preferential population of bridge sites while CO prefers the top sites in the absence of K. This then, would be an example of an electronic effect that influences the bonding geometry as well.[5]

In order to explore the molecular basis of the effects of alloying on the catalytic activity we carried out reaction rate studies on well characterized single crystal surfaces with known atomic structure and composition. We report here studies of the Pt-Au system. Gold was evaporated onto the (111) crystal face of platinum to form either an epitaxial overlayer or an alloy system. The system was characterized by low energy electron diffraction (LEED) and Auger electron spectroscopy (AES). Temperature programmed desorption (TPD) of carbon monoxide was also carried out as a function of gold surface concentration as the CO desorption was found to be sensitive to the surface structure of the Pt(111)-Au system. Catalytic studies were carried out using n-hexane, that undergoes several different reactions over platinum: dehydrogenation, isomerization, dehyaromatization, C_5-cyclization and hydrogenolysis. The experiments were carried out in an ultrahigh vacuum (UHV) apparatus equipped with a sample isolation cell. In this way, surfaces could be prepared and characterized under UHV conditions with subsequent reaction studies <u>in situ</u> at pressures of the order of 1 bar. The bimetallic surfaces were prepared by vapor deposition of Au onto the Pt(111) substrate, in some cases followed by a high temperature treatment.

It was found that gold overlayers deposited at 300 K uniformly covered the various platinum surface sites without altering their relative concentrations. As gold was allowed to diffuse into the Pt surface by high temperature annealing to an the alloy the large Pt ensembles were drastically reduced with a profound effect on the catalytic properties. The surfaces with only small Pt ensembles were more active than pure platinum and had a high selectivity for isomerization, while surfaces with unaltered site distribution behaved as pure Pt(111) with a reduced surface area. The ligand or electronic effect was shown to be insignificant for the Au-Pt(111) system studied here as could be judged by studies of the chemisorption of CO. However, changes of bonding of organic molecules was induced by alteration of the Pt(111) surface structure by alloying that markedly altered the activity and the selectivity of the catalyst.

2. EXPERIMENTAL

2.1 Apparatus

The experiments were carried out in an UHV system equipped with a sample isolation cell to permit in-situ reaction studies at pressures of up to 1 bar.

Surface characterization was accomplished with four-grid LEED optics that were also used to collect and energy analyse the Auger electrons which were generated by irradiating the sample with a separate electron gun. A quadrupole mass spectrometer was used for TPD measurements.

The bimetallic surfaces were prepared by vapor deposition of Au onto a Pt(111) single crystal surface. The effusive type gold source was located in a separate, differentially pumped chamber. The evaporation geometry was the same as in earlier studies.(6)

The platinum single crystal was spotwelded to very short pieces of 0.5 mm ϕ Pt wire spotwelded to 0.8 mm ϕ Au wires which in turn were pressed inside

matching holes of the Cu feedthroughs. This arrangement is shown in reference 7 but thinner mounting wires had to be used here. Very even heating without hot spots was assured this way. In order to shorten cooling times after annealing or TPD measurements, the crystal was cooled through the electrical leads by immersing copper bars mounted on the electrical feedthroughs, in liquid nitrogen. This also lowered the adsorption temperatures to 250-270 K. The crystal temperature was measured with a chromel-alumel thermocouple spotwelded to its edge.

Details of the sample isolation cell are described in reference 8. Briefly, the crystal was mounted as described from feedthroughs in a small disk that itself was attached to the manipulator. By raising the movable part of the isolation cell against this disk, the single crystal would become enclosed in a small volume that was sealed from the surrounding UHV. In this apparatus a Viton O-ring was used instead of a gold gasket as in reference 8. Reaction studies could then be performed by passing reactants through this volume and heating the crystal to reaction temperature. The gases were circulated with a teflon gear pump and samples were taken with a gas sampling valve and analyzed by a gas chromatograph with a flame ionization detector. The system operated this way as a well-stirred batch reactor with a volume of 0.165 liter.

2.2 Materials

The Pt(111) single crystal was prepared by spark erosion of a thin wafer from a high purity single crystal rod (within 1° of the (111) orientation as determined by Laue back reflection X-ray diffraction). This wafer was polished mechanically on both sides and etched very briefly in aqua regia before mounting in the vacuum chamber. The hydrocarbons used in these experiments were n-hexane (obtained from Phillips Petroleum Company) and trans hexene-2 (obtained from Aldrich Company). The purity of the n-hexane was found to be 99.95 mole%,

by gas chromatographic analysis, with predominantly methylcyclopentane and also some benzene and 3-methylpentane as contaminants. The purity of the trans hexene-2 was found to be 99.9 mole% with pentane-2, cis hexene-2 and 2- and 3-methylpentane as major impurities. The hydrocarbons were degassed by repeated freeze-pump-thaw cycles. The high purity hydrogen obtained from the Lawrence Berkeley Laboratory was passed through a molecular sieve trap before use.

2.3 Procedures

After more severe treatments to remove impurities that were initially present in the new single crystal, the following cleaning procedure was routinely used. First the front and back surfaces were argon ion bombarded (6.7×10^{-5} mbar (5×10^{-5} Torr), 1 keV ions) for 30 minutes each, at 295 K. In this way the surface region from the previous experiment was completely removed, preventing the accumulation of Au in the bulk of the Pt crystal. After annealing for 15 minutes at 1250 K residual carbon was removed in 6.7×10^{-7} mbar (5×10^{-7} Torr) O_2 at 1150 K for 40 seconds or less, followed by desorption of any remaining oxygen at 1250 K for 3 minutes. Then the crystal was cooled and surface cleanliness was checked with AES. If necessary, the oxygen treatment was repeated. The resulting surfaces were clean according to AES and produced LEED patterns with sharp spots. In order to produce an epitaxial surface, gold was deposited in equal amounts onto each crystal face, at 295 K. The accumulation of Au was monitored with AES.

When a surface alloy had to be studied, the clean Pt(111) surface was additionally characterized by a TPD spectrum of CO, after saturation exposure of 36 L (1 L = 1.3×10^{-6} mbar•s (1×10^{-6} Torr•s)) at 250-270 K. Then 3-4 monolayers of gold were deposited on each crystal face followed by a thermal treatment consisting of one or more flashes to 1100-1250 K to cause interdiffusion of the Au and Pt. The decrease of the gold surface concentration was followed

by AES and after cooling to 250-270 K a TPD spectrum of CO was recorded, after 36 L exposure.

Next the sample isolation cell was closed and 26.7 mbar n-hexane were introduced, followed by 267 mbar hydrogen. After circulating the gases for 10 or 20 minutes respectively, with the crystal at room temperature, two samples were taken to verify the gas composition and the absence of background activity. Three minutes after the reaction was started by heating the crystal to the reaction temperature of 573 K, another sample was taken followed by more at 10 minute intervals, for the duration of the reaction. After the reaction time of 3 hours the crystal was cooled in the reaction mixture and the reactor was evacuated. Finally, the cell was opened and the surface reexamined. As the sample isolation cell was setup as a batch reactor, kinetic data were obtained in the form of product accumulation curves. Using the surface area of the Pt(111) sample crystal that was measured geometrically (0.7 cm^2) the amounts of product were calculated as molecules formed per surface atom. Unless otherwise specified, data in this paper were calculated per total number of surface atoms, Pt + Au. Initial rates were obtanied by graphically determining the initial slopes of accumulation curves. The fission parameter, M_f, characterizing the hydrogenolysis product distribution, was calculated in the usual way.(9) The amounts of hydrogenolysis products were calculated as the number of hexane (or hexene) molecules consumed, except for the hydrogenolysis product distributions where molefractions were used. The experiments in which aromatization was studied were carried out separately as a different column had to be used in the gas chromatograph for the separation of benzene.

The TPD spectra were measured by the quadrupole mass spectrometer, upon heating the crystal at a rate of 68 K s^{-1}. During CO adsorption, the crystal temperature was 250-270 K. Separation of the overlapping Au and Pt Auger transi-

tions, determination of the film growth mechanism of Au deposited on the Pt(111) surface and calibration of the gold coverages were carried out according to the procedures described in reference 6 for Au on Pt(100).

3. RESULTS

3.1 Surface Characterization with AES and LEED

3.1-1. Epitaxial Au layers on Pt(111)

As has been discussed in the literature,[10] and studied in detail with the Au on Pt(100) and Pt on Au(100) systems,[6] AES can be used to determine the growth mechanism of the metal that is deposited onto the surface of another metal. In order to obtain this information, an Auger signal versus time of deposition (ASt) plot has to be generated. The various growth mechanisms show characteristic features in their ASt plots through which they may be identified. With the current system this analysis is complicated by the overlap of Au and Pt Auger transitions, as is evident from Figure 1 where Auger spectra are shown recorded after various times of deposition of Au on Pt(111), at 295 K. After applying the peak separation following reference 6 an ASt-plot could be constructed and the result is shown in Figure 2. It should be noted that under conditions of constant deposition rate as used here, the deposition times are preportional to the Au coverages.

Careful inspection of the data plotted in Figure 2 reveals three breaks, at deposition times of 13.0, 27.0 and 39.5 minutes. An observation of multiple breaks at times obeying the ratio 1:2:3 as expected for a successive completion of three monolayers, indicates a layer-by-layer (Frank-van der Merwe) growth mechanism. The data in Figure 2 could also be described numerically with the layer-by-layer growth mechanism unsing the Gallon model[11] and the calculated curve that gave the best fit is shown by the solid lines in Figure

2. Using the monlayer deposition time of 13.2 minutes obtained from the positions of the breaks, optimization of the fit gave a normalized monolayer Auger intensity $I(1)/I(\infty) = 0.55$ and a variance (sum of squares of the differences between calculated and experimental values) $V = 0.0038$. The parameter $I(1)/I(\infty)$ is related to the mean free path, λ, of the Auger electrons[12] and using an interlayer spacing of 2.226nm (based on the bulk Pt lattice constant of 0.39239nm[15]), a value of $\lambda = 0.38$nm was calculated.[10] It should be noted that determination of the monolayer deposition time automatically also provides the coverage calibration of the Auger spectra.

LEED observations of these surfaces revealed the following. The clean Pt(111) surface showed the expected hexagonal diffraction pattern. Upon deposition of Au this pattern was always retained. Submonolayer amounts of gold, as well as multilayers, did not lead to any new spots, even after annealing at temperatures as high as 1270 K. The sharpness of the diffraction spots did, however, appear to decrease slightly after several layers of Au had been deposited.

From measurements of spot-spot distances in LEED patterns obtained at different Au coverages, changes in the surface lattice constant have been calculated. The accuracy of these measurements was limited by the sizes of the diffraction spots which were significant compared to the 4% difference in bulk lattice constants of Au and Pt (0.40785nm and 0.39239nm respectively[13]). Within the accuracy of these measurements of about 1% of a lattice constant, a continuous increase of the lattice constant of the clean Pt(111) surface towards that of Au(111) was found, spread out over about five or more monolayers. One monolayer of Au on Pt(111) had the same lattice constant as the substrate, within experimental accuracy, and was clearly contracted as compared with the bulk value.

3.1-2. Surface Alloys

AES was used to follow the decrease of the amount of Au at the surface upon annealing but it was not used for quantitative determination of the Au and Pt surface concentrations, or the depth profile of the composition was not known (see also 3.2-3).

LEED observations of a series of alloy surfaces that were generated by heating the Pt(111) single crystal covered with a multilayer Au deposit for various lengths of time to increasing temperatures, showed that in all cases the alloy surfaces were well ordered with the same geometry as the Pt(111) substrate. Extra spots, indicative of reconstruction or of the formation of new surface structures were not observed.

3.2 Surface Characterization with TPD of CO

3.2-1. Clean Pt(111)

A series of TPD spectra recorded after various exposures is shown in Figure 3. Only one peak is observed with a peak maximum temperature, T_m, that shifts to lower values with increasing exposure. This variation is presented explicitly in Figure 4. From these values the activation energy for desorption, E_d, can be calculated using Redhead's equation for first order desorption kinetics.[14] Assuming a pre-exponential factor of $10^{13}s^{-1}$, a value of E_d = 116 kJ/mole is obtained after extrapolation to zero coverage. This value is in good agreement with literature values of 117,[15] 124[16] and 113 kJ/mole.[17] The decrease of T_m from 490 to 415K with increasing CO exposure (Figure 4) can be explained by repulsive interactions between the adsorbed CO molecules because of crowding that increases with increasing coverage weakening and weakens the CO-Pt bonds. Because of this dependence, T_m can be used as a measure of the average CO-CO distance in the adsorbed layer. This interpretation is of importance for the analysis of TPD spectra from the bimetallic sur-

faces.[18]

3.2-2. Epitaxial Au on Pt(111)

Figure 5 shows the TPD spectra of CO from the Pt(111) surface that was covered with various amounts of Au deposited at 295 K. All desorption traces were recorded after 36 L exposures, high enough to saturate the surface with adsorbed CO molecules. There are two major observations; (1) the temperature, T_m, of the maximum rate of desorption does not change with gold coverage and remains the same (415 K) as obtained on the clean Pt(111) face at high CO coverages. This is shown in Figure 6. This indicates the presence of large patches of uncovered Pt(111) where neighboring CO molecules can exert their repulsive interaction. (2) There is a linear reduction in the amount of CO adsorbed with gold coverage. This is shown in Figure 7. The position of the break in Figure 7 which indicates the completion of the first monolayer is in excellent agreement with the coverage that was determined from the ASt plot. After heating the gold covered surface to 700 K, the highest temperature of the TPD spectra, a peak at about 470 K was observed. Apparently this new state in Figure 5 is due to diffusion of substrate Pt atoms through the Au layer at the elevated temperatures of the TPD measurements.

The other new feature of Figure 5 is a low temperature shoulder that is not an artifact. It was observed that this shoulder decreased in intensity in a second desorption measurement on the same surface, to which not more Au had been added. At the elevated temperatures of the temperature ramp, faster surface diffusion and aggregation of Au into larger two-dimensional islands would be possible. These larger islands would have a smaller total circumference which would explain the observations if this desorption state is due to CO chemisorbed on Pt atoms next to the step formed by a gold island boundary. In this paper the amounts of CO desorbed will be presented as normalized yields

which are defined as the area under desorption curves divided by the area under the desorption curve for clean Pt(111) after saturation exposure of 36 L. In order to maximize reproducibility a new Pt(111) reference TPD spectrum was measured at the beginning of every experimental sequence.

As TPD of CO is able to detect very small ammounts of Pt, this technique was also used to investigate the stability of a gold layer at the reaction temperature of 573 K. The TPD spectrum of the Pt(111) surface covered on each side by 1.2 monolayers of Au only showed the featureless broad peak characteristic of the edges of the crystal. After heating to 573 K for 11.8 hours a small alloy desorption peak was found on top of this background desorption. The desorption yield of this peak was only 0.1% of that of clean Pt(111) which demonstrates the high stability of the epitaxial layer at this temperature.

3.2-3. Au-Pt(111) surface alloys

When CO was adsorbed to saturation coverage on the Au-Pt(111) alloys the maximum desorption rate occurred at higher temperatures than on the epitaxial Au-Pt(111) surfaces. This is shown, as a function of gold surface concentration, in Figure 8. On the alloy surface, T_m approaches the value (490 K) that is obtained for the clean Pt(111) surface at low CO coverages when repulsive interactions among the CO molecules do not weaken the CO-Pt bond. Thus, it appears, that in the alloy the gold atoms do not permit the crowding of the CO molecules that, therefore, maintain their higher binding energy to the platinum atoms. Apparently gold atoms in the alloy break up the available platinum surface into small ensembles that can no longer adsorb a dense layer of CO molecules in which repulsive interactions lower T_m from 490 to 415K. Gold alloying has the effect of preventing the crowding of CO molecules by creating small platinum islands that can only be sparsely populated with CO. In conclusion, T_m when determined by CO desorption after 36 L exposures from the epitaxial

gold-Pt(111) and gold alloy-Pt(111) systems reveals that (a) there are large platinum ensembles present in the surface of the partially gold covered epitaxial system while only small platinum ensembles are available in the surface of the Au-Pt(111) alloy.

3.2-4. The absence of the ligand effect for CO adsorption in the Au-Pt(111) system

It is possible that upon alloying T_m does not only change due to geometrical separation of the CO molecules, but also because of a change in the intrinsic bonding abilities of a Pt atom when its Pt neighbors are replaced by Au. In order to investigate this effect the surfaces have to be studied under conditions where the influence of CO-CO interactions has been eliminated. One way of doing this is by going to the limit of zero CO coverage. Then, chemisorption bond strengths can be compared of a single CO molecule on a clean Pt(111) surface and a single CO adsorbed on a Pt atom that is surrounded by Au neighbors. (According to the literature, at low coverages CO on Pt(111) is adsorbed in on-top sites[19]). The difference in T_m between these two cases will then indicate the importance of the ligand effect. Figure 9 shows the relevant observations. For clean Pt(111) the variation of T_m with CO coverage was obtained by varying the CO exposure. Going to very low exposures, which corresponds to going to the left in Figure 9, a sudden increase of T_m is observed that cannot be explained by decreasing CO interactions as this effect should level off. The sudden rise is then attributed to imperfections of the single crystal surface that bind CO more strongly than terrace Pt atoms.[20] At the lowest exposures, only these sites are populated. In order to eliminate these effects the middle range of the data was extrapolated to zero CO coverage. For the alloys, exposures were always at the saturation value of 36 L. Extrapolation of the alloy data to zero yield gives T_m for a single CO adsorbed on a

surface platinum atom with only Au neighbors. As Figure 9 shows the two cases give the same T_m within the experimental error of about 5 K. This error bar of 5 K only corresponds to a difference in adsorption energy of 1.2 kJ/mole which is insignificant compared to the 16.7 kJ/mole coverage induced variation of the chemisorption bond strength.

3.3 Conversion of n-Hexane

Under the reaction conditions used in this work, n-hexane was converted to cis- and trans-hexene-2, 2- and 3-methylpentane (2MP, 3MP), methylcyclopentane (MCP), smaller hydrocarbons ($\Sigma < C_6$) and benzene (BZ). The cis- and trans-hexene-2 were the only olefins that could be detected. The kinetic data were obtained as product accumulation curves of which two examples are shown in Figure 10a and b. The kinetics of the hexene-2 formation could not be followed as the first data points were already close to the hexane/hexene equilibrium, particularly in the case of gold containing surfaces where olefin formation was enhanced. Initial selectivities were calculated from the initial rates which were determined by graphical determination of the initial slopes of the accumulation curves. As is evident from figure 10, steady state rates were not reached due to selfpoisoning. "Integrated" selectivities were calculated from the amounts of products accumulated in two hours of the reaction.

3.3-1. Epitaxial Au layers on Pt(111)

Initial rates of formation of 2- and 3MP, MCP, $\Sigma < C_6$ and BZ are plotted against gold surface coverage in Figure 11. All measurements were performed at very low conversion levels (see Figure 18). It should be mentioned that in this Figure, as in Figure 12, 15 and 18, initial rates have been calculated per total number of surface atoms, i.e. Pt + Au. As it was experimentally not possible to cover the crystal edges with gold, some activity remained at high gold coverages. Thus, a linear decrease of the rate of formation from zero to monolayer

Au coverage, followed by a low but constant level of activity indicates that the turnover frequency per platinum surface atom is actually constant. As Figure 11 shows this was the case for aromatization and hydrogenolysis. Isomerization and C_5-cyclization, of which it is known that they may have the same precursor,[21] showed a different behavior. However, the sum of the latter reaction rates did show the same linear coverage dependence (Figure 12). This can be understood if at least a part of MCP and 2- and 3MP was indeed formed through a common intermediate. The linear decrease of the total amount of products and consequently also of the amount of intermediate formed, reflects the decrease of available Pt(111) surface area with increasing Au coverage. Additionally, Au apparently shifted the selectivity of product formation from the intermediate towards isomerization, at the expense of MCP. The selectivities that were calculated from the initial rates, after correction for edge contributions, are shown in Figure 13.

3.3-2. Separation of face and edge contributions to the total n-hexane conversion and CO desorption

An additional benefit from the study of epitaxial gold layers on a single crystal surface of an active metal is that face and edge contributions can be separated. The edges expose a multitude of crystal orientations and often contain impurities in the surface as they are at least partially shadowed during argon ion cleaning, and consequently they may have different properties than the front and back faces of the crystal. Thus, they may perturb reactivity and TPD reuslts. However, when the polished crystal faces are covered by Au, the edges remain uncovered and their activity can thus be identified and used to correct the results. As Figure 11 shows, the edges are rather unimportant for the reuslts shown there. However, the crystal edges are quite different in their hydrogenolysis product distribution. As is shown n Figure 14, the

edges produce predominantly methane while the clean, well oriented (111) surfaces also give substantial amounts of propane. Without subtracting the edge contribution, too low a value of the fission parameter, M_f, would have been obtained for the Pt(111) surface.

3.3-4. Au-Pt(111) surface alloys

Figure 15 shows the gold surface concentration dependence of the initial rates of formation of the products from the n-hexane reaction, catalyzed by surface alloys. The most striking feature is the increase of the isomerization rate, when active Pt atoms are replaced by inactive Au. The increase of the isomerization activity is already seen by comparing Figures 10a and b where the data is presented in the form of accumulation curves. Aromatization and hydrogenolysis are inhibited by the addition of gold while C_5-cyclization shows a roughly linear decline with gold concentration. In Figure 16 the same results are shown, but now the rates have been calculated per Pt surface atom, after correction for edge contributions. In this case, possible inaccuracies of the determination of the surface composition have been included in the rates, unlike in Figure 15. Also, the scatter of the data becomes magnified at high gold coverages, in Figure 16. The addition of gold to Pt(111) as epitaxial islands also caused some enhanced isomerization but the differences between the two types of surfaces are significant as can be seen in Figure 13. A major difference is that the selectivity effects of the epitaxial surfaces were only transient while alloying with Au changed the nature of the surface permanently. This becomes evident from Figure 17 where the "integrated" selectivities for both systems are plotted against surface gold concentration. Here, the epitaxial Au islands show no modification of the Pt(111) properties while the alloys clearly exhibit enhanced isomerization. Figure 18 demonstrates that not only the integrated selectivities, but also the cumulative activities after two

hours of reaction of the alloys are different from those of the epitaxial surfaces. As the latter behave as pure Pt(111) surfaces with reduced surface area, it is concluded that the alloys are always more active than pure Pt(111) with the same active metal surface area. It should be mentioned, that the Au and Pt surface concentrations are not altered during the reaction, within the accuracy of AES.

3.3-4. Formation of a carbonaceous overlayer during reaction

During hydrocarbon reactions strongly bound, (partially) dehydrogenated fragments are formed on the catalyst surface. In the apparatus used here, after reaction the cell could be opened and the surface could be examined again with LEED and AES. Becuase of the UHV environment, only strongly bound species will remain on the surface. LEED observations after reaction did not show a pattern, indicating the absence of an ordered overlayer. AES could be used to determine the amount of carbon on the surface and the results are shown in Figure 19. Neither these data, nor the LEED observations, were altered by heating the surface in vacuum to 573 K before the surface characterization. An Auger peak intensity ratio of the 272 eV carbon and 237 eV platinum transitions of 3.2 was used to identify one carbon monolayer,[22] which has been shown to contain two carbon atoms per surface atom.[23] Since the Au and Pt Auger spectra are very similar and in this energy range practically identical, the same carbon coverage calibration was used for Au containing surfaces. As the data in Figure 19 are quite scattered, a gray shaded area is used to indicate the range that covers most of the results for the epitaxial surfaces. It should be noted that even on Au multilayers which are also plotted in the Figure (at a fractional gold surface coverage of unity), carbon deposition occurred. Separate experiments of the same reaction under the same reaction conditions with a pure Au single crystal proved that carbon deposition on gold does indeed occur. The

alloy values seem to be lower than the epitaxial ones, but the significance of this difference is uncertain.

4. DISCUSSION

4.1 The Presence of Small Pt Clusters in the Pt-Au Alloy Surfaces and of Large Pt Clusters in the Pt-Au Overlayer Surfaces

Temperature programmed desorption of CO provides important information on the nature of the bimetallic surfaces. The temperature T_m has been found to be sensitive to the distribution of platinum atoms in the surface. This interpretation is based on the variation of T_m with CO coverage on the clean Pt(111) surface. With increasing coverage the distances between adsorbed CO molecules decrease, increasing their mutual repulsive interactions and thus lowering the activation energy for desorption.

When the Pt atoms in the surface remain as fairly large contiguous arrrays (large ensembles) CO molecules can still be packed as closely as is permitted by the repulsive interactions, and these large ensembles will behave as clean Pt(111) surfaces. This is the case for epitaxial gold layers on top of platinum. However, when the Pt atoms are randomly distributed in the surface as in the Au-Pt alloys this will no longer be the case. Then, with increasing gold concentration the probability of finding large ensembles will decrease more rapidly than the chance of finding small ensembles. Consequently, with increasing Au concentration the average ensemble size will decrease. Although a distribution of ensemble sizes exists at any given surface composition, this discussion will be held in terms of average ensemble size as this is the quantity that is reflected by the experimentally obtained parameter T_m. As the ensembles become smaller, fewer CO molecules will be adsorbed per ensemble, reducing on the aver-

age the number of neighbors that every CO molecule can interact with. The interactions with CO molecules on other ensembles will be weaker since the ensembles are spatially separated by Au. Thus, the adsorption energy of CO will increase with increasing Au surface concentration in the case of the Au-Pt alloy where Au and Pt are randomly distributed in the surface.

A new desorption state with a lower binging energy was observed on the epitaxial surfaces. This state was attributed to the edges of the Au islands and may be caused by steric hinderance by a gold-step on the bonding of CO to an adjacent Pt atom. However, this state is much less populated than the state corresponding to the main peak and does not affect T_m.

The picture of the epitaxial surfaces is one of two-dimensional Au islands that leave large patches of platinum uncovered which retain their Pt(111) character. Only adsorption on Pt atoms adjacent to the edges of a Au island is somewhat perturbed.

LEED observations of both the alloy and the epitaxial Pt-Au surfaces showed that they were all well ordered and had (1 x 1) surface structures. Thus, they did indeed represent (111) oriented surfaces.

4.2 n-Hexane Conversion Over Pt-Au Alloy and Pt-Au Overlayer Surfaces

The results of the n-hexane conversion demonstrate that the two types of surfaces have different catalytic properties and we ascribe this to the differences in ensemble size. Van Schaik et al.[24] reported that upon alloying platinum with gold, the selectivity for hydrogenolysis declined rapidly, dehydrocyclization showed a maximum and then decreased, while the selectivity for isomerization increased. These experiments were carried out in a flow reactor at a total pressure of 1 bar, using SiO_2 supported particles. The good agreement of these findings with the "integrated" selectivites obtained in our work (Figure 17) supports the expectation that our results can be compared with

results obtained under steady state conditions using supported Au-Pt alloy catalysts.

There is, however, one major difference between results from this work and those in reference 24. The Au-Pt alloys in this work having small platinum clusters were always more active than surface where the same amount of Pt was arranged in larger ensembles (Figure 18). In the study reported by Van Schaik et al. all reaction rates involving C-C bond rearrangements were found to always decrease with increasing concentration of the Ib metal,Au. Selectivity changes occurred because some of the reactions were inhibited more strongly than other reactions.

There is a number of possible explanations for the surprising activity-enhancment observed for the Au-Pt alloys in our studies.

a) In our work great care was taken to characterize the surfaces and the observed rate enhancement effects are definitely significant. In the study of the supported Pt-Au system,[2b,24] the absolute rates were not determined as rates were only determined per unit weight of per unit total (B.E.T.) surface area of the catalysts without selective determination of the surface area of the active metal component. One possible explanation for the apparent differences between our work and the literature data is, therefore, that in the latter the active surface areas were overestimated.

b) In a complex reaction system as with n-hexane many reactions occur at the same time and the possibility has to be considered that the effect of alloying operates indirectly by affecting competing side reactions.

Gold was found not only to enhace isomerization, but also dehydrogenation. If 2- and 3MP are formed from hexene-2, the enhanced olefin formation would cause more isomerization as well. There are, however, two pieces of evidence against this case. First, olefin formation is not only enhanced with the

alloys, but also with the epitaxial surfaces. Enhanced isomerization, however, was only pronounced with the alloys. Second, using pure hexene-2 as reactant did not increase the production of 2- and 3MP.

Another side reaction that should be considered is the formation of a strongly bound carbonaceous layer on the surface, blocking reaction sites. If the formation of this layer requires large ensembles, this would be suppressed on alloy surfaces where then more Pt atoms would be available for reaction than on a largely carbon covered Pt(111) surface. Unfortunately, the AES measurements of the amounts of carbon deposited by the reaction (Figure 19) are too scattered to decide this definitively.

c) The small Pt ensembles may have higher activity than the large Pt ensembles. For the isomerization of pentanes and hexanes high negative reaction orders in hydrogen are found which are currently interpreted by assuming that the rate-determining step is the skeletal rearrangement of highly dehydrogenated species.[25] When Pt is alloyed with Au the extent of dehydrogenation of the reaction intermediates may well be less due to the limited number of Pt atoms available in small ensembles. A higher activity of these less dehydrogenated and thus less strongly bound species could explain the observed isomerization increase.

This argument does not, however, explain the intermediate behavior of MCP in Figure 15. MCP and 2- and 3MP may both be formed through a common "C_5-cyclic" intermediate and O'Cinneide et al. have shown that the fraction of isomerization products formed through this intermediate is larger with Pt-Au alloys than with pure Pt.[21b] With the epitaxial surfaces we found that the initial enhancement of isomerization occurred at the expense of MCP formation. Thus, the intermediate behavior of MCP formation on the surface alloys can be rationalized as a compensation of the enhanced production of intermediates by a

decreased selectivity of these species for MCP formation. Consequently the enhanced isomerization would actually be due to the constructive addition of both these effects.

Judging by TPD, the bonding of CO to the Pt-Au alloy and overlayer surfaces is identical to that to the clean Pt(111) surface. The only important effect is the coverage dependence of the heat of adsorption which permitted us to identify the presence of small Pt clusters in the Pt-Au alloy surfaces and of large Pt clusters in the Pt-Au overlayer surfaces. The presence of ligand or electronic effects on the changes of bonding n-hexane or certain reaction intermediates that form during the conversion of n-hexane to the various products cannot be ruled out, however. The enhancement of the isomerization rate must be due to changes of bonding that are induced either by charge redistribution or by structural changes as small Pt clusters of (111) orientation are produced.

More studies that systematically vary the platinum surface structure and the alloying IB constituent (Cu and Ag instead of Au) are needed to verify the causes of this interesting reaction rate enhancement effect.

5. CONCLUSIONS

1) Deposition of Au on Pt(111) near 300 K produces an epitaxial Au layer consisting of two-dimensional islands that leave large ensembles of Pt(111) uncovered. With increasing coverage, the islands grow until the monolayer is completed, before the second layer begins to form.

2) High temperature annealing of Pt(111) surface covered by several layers of gold produces a surface alloy with small Pt ensembles.

3) The temperature of the maximum rate of desorption in the TPD spectra of CO is sensitive to the Pt ensemble sizes.

4) The ligand effect was found to be insignificant for CO adsorption on the Au-Pt(111) alloys.

5) The alloy surfaces are more active than the corresponding monometallic surfaces with the same Pt content.

6) The ensemble size has a profound influence on the n-hexane skeletal reactions. The small Pt clusters present in the Au-Pt alloys exhibit enhanced isomerization rates and reduced hydrogenolysis and aromatization rates as compared to clean Pt(111) or Pt-Au overlayer surfaces with large Pt clusters.

ACKNOWLEDGMENT

This work was supported by the Director, Office of Energy Research, Office of Basic Energy Sciences, Materials Sciences Division of the U.S. Department of Energy under Contract DE-AC03-76SF00098.

REFERENCES

1a. V. Ponec, Catal. Rev.-Sci. Eng. 11(1), 41 (1975);

1b. J.K.A. Clarke, Chem. Rev. 75, 291 (1975);

1c. J.H. Sinfelt, Accts. Chem. Res. 10, 15 (1977);

1d. W.M.H. Sachtler and R.A. van Santen, Advan. Catal. 26, 69 (1977);

1e. V. Ponec, Surf. Sci. 80, 352 (1979);

1f. H.C. de Jongste and V. Ponec, Bull. Soc. Chim. Belg. 88(7-8), 453 (1979).

2a. W.M.H. Sachtler, Le Vide 164, 67 (1973);

2b. V. Ponec and W.M.H. Sachtler, J. Catal. 24, 250 (1972).

3. Y. Soma-Noto and W.M.H. Sachtler, J. Catal. 32, 315 (1974).

4a. J.J. Stephan, V. Ponec and W.M.H. Sachtler, Surf. Sci. 47, 403 (1975);

4b. J.R. Anderson, K. Foger and R.J. Breakspere, J. Catal. 57, 458 (1979).

5. E.L. Garfnkel, J.E. Crowell and G.A. Somorjai, J. Phys. Chem. 86, 310 (1982).

6. J.W.A. Sachtler, M.A. Van Hove, J.P. Biberian and G.A. Somorjai, Surf. Sci. 110, 19 (1981).

7. R.K. Herz, W.D. Gillespie, E.E. Petersen and G.A. Somorjai, J. Catal. 67, 371 (1981).

8. J.C. Hemminger, R. Carr and G.A. Somorjai, Chem. Phys. Lett. 57(1), 100 (1978).

9. V. Ponec and W.M.H. Sachtler, Proc. Int. Congr. Catal. 5th, 1972, Pap. 43, pg. 645 (1973).

10. G.E. Rhead, J. Vac. Sci. Technol. 13(2), 603 (1976).

11a. T.E. Gallon, Surf. Sci. 17, 486 (1969);

11b. D.C. Jackson, T.E. Gallon and A. Chambers, Surf. Sci. 36, 381 (1973).

12. M.P. Seah, Surf. Sci. 32, 703 (1972).

13. Handbook of Lattice Spacings and Structures of Metals, Vol. 2, Ed. W.B. Pearson, Pergamon, London (1967).

14. P.A. Redhead, VAcuum 12, 203 (1962).

15. G. Ertl, M. Neumann and K.M. Streit, Surf. Sci. 64, 393 (1977).

16. R.W. McCabe and L.D. Schmidt, Surf. Sci. 66, 101 (1977).

17. D.M. Collins and W.E. Spicer, Surf. Sci. 69, 85 (1977).

18. W.M.H. Sachtler, J. Vac. Sci. Technol. 9(2), 828 (1971).

19a. H. Froitzheim, H. Hopster, H. Ibach and S. Lehwald, Appl. Phys. 13, 147 (1977);

19b. H. Hopster and H. Ibach, Surf. Sci. 77, 109 (1978).

20. D.M. Collins and W.E. Spicer, Surf. Sci. 69, 85 (1977).

21a. F.G. Gault, Advan. Catal. 30, 1 (1981);

21b. A. O'Cinneide and F.G. Gault, J. Catal. 37, 311 (1975).

22. J.P. Biberian and G.A. Somorjai, Appl. Surf. Sci. 2, 352 (1979).

23. S.M. DAvis, B.E. Gordon, M. Press and G.A. Somorjai, J. Vac. Sci. Technol. 19(2), 231 (1981).

24. J.R.H. Van Schaik, R.P. Dessing and V. Ponec, J. Catal. 38, 273 (1957).

25. F.G. Gault, V. Amir-Ebrahimi, F. Garin, P. Parayre and F. Weiseng, Bull. Soc. Chim. Belg. 88(7-8), 475 (1979).

FIGURE CAPTIONS

Figure 1. Auger spectra of Pt(111) covered with various amounts of Au. "t" indicates deposition time, in minutes, at constant evaporation rate.

Figure 2. Auger signal versus time plot of Au on Pt(111).

Figure 3. TPD spectra of CO adsorbed on Pt(111), as a function of exposure.

Figure 4. Variation of the desorption peak temperature with CO exposure. (1 L = 1 Langmuir = 1.3×10^{-6} mbar s (1×10^{-6} Torr s)).

Figure 5. TPD spectra of CO adsorbed on Pt(111) covered with varying ammounts of gold, after constant saturation exposure of 36 L.

Figure 6. Variation of the desorption peak temperature, after constant saturation exposure of 36 L, with gold coverage on Pt(111).
: Pt(111) surface covered with submonolayer amounts of gold.
: Pt atoms that diffused through the Au layer, an artifact of these measurements.

Figure 7. Variation of the normalized desorption yield, after constant saturation exposure of 36 L, with gold coverage on Pt(111).

Figure 8. Variation with surface gold contents of the desorption peak temperature, after saturation exposure of 36 L, for epitaxial and alloy surfaces.

Figure 9. Variation of the desorption peak temperature with normalized CO desorption yield, for clean Pt(111) and alloy surfaces.

Figure 10. Product accumulation curves for n-hexane reactions.
(a) Clean Pt(111) surface.
(b) Alloy surface with platinum surface concentration of 29 atom %.

Figure 11. Gold coverage dependence of the initial formation rates of products from the n-hexane reaction catalyzed by the epitaxial surfaces.

Figure 12. Sum of rates of formation of methylcyclopentane and 2- and 3-methylpentane as a function of gold coverage.

Figure 13. Initial product selectivities of the n-hexane conversion catalyzed by epitaxial and alloy surfaces.

Figure 14. Hydrogenolysis product distribution for the Pt(111) surface (corrected for edge contributions) and for the crystal edges.

Figure 15. Gold surface concentration dependence of the initial formation rates of products from the n-hexane reaction catlayzed by surface alloys.

Figure 16. Variation of reaction rates calculated per platinum surface atom, with alloy gold surface concentration.

Figure 17. "Integrated" product selectivities of the n-hexane conversion calculated using amounts of product accumulated in two hours of the reaction.

Figure 18. Conversion of n-hexane in two hours of reaction as a function of surface gold concentration for epitaxial and alloy surfaces.

Figure 19. Amounts of strongly bound carbon deposited on the epitaxial and alloy surfaces in three hours of reaction.

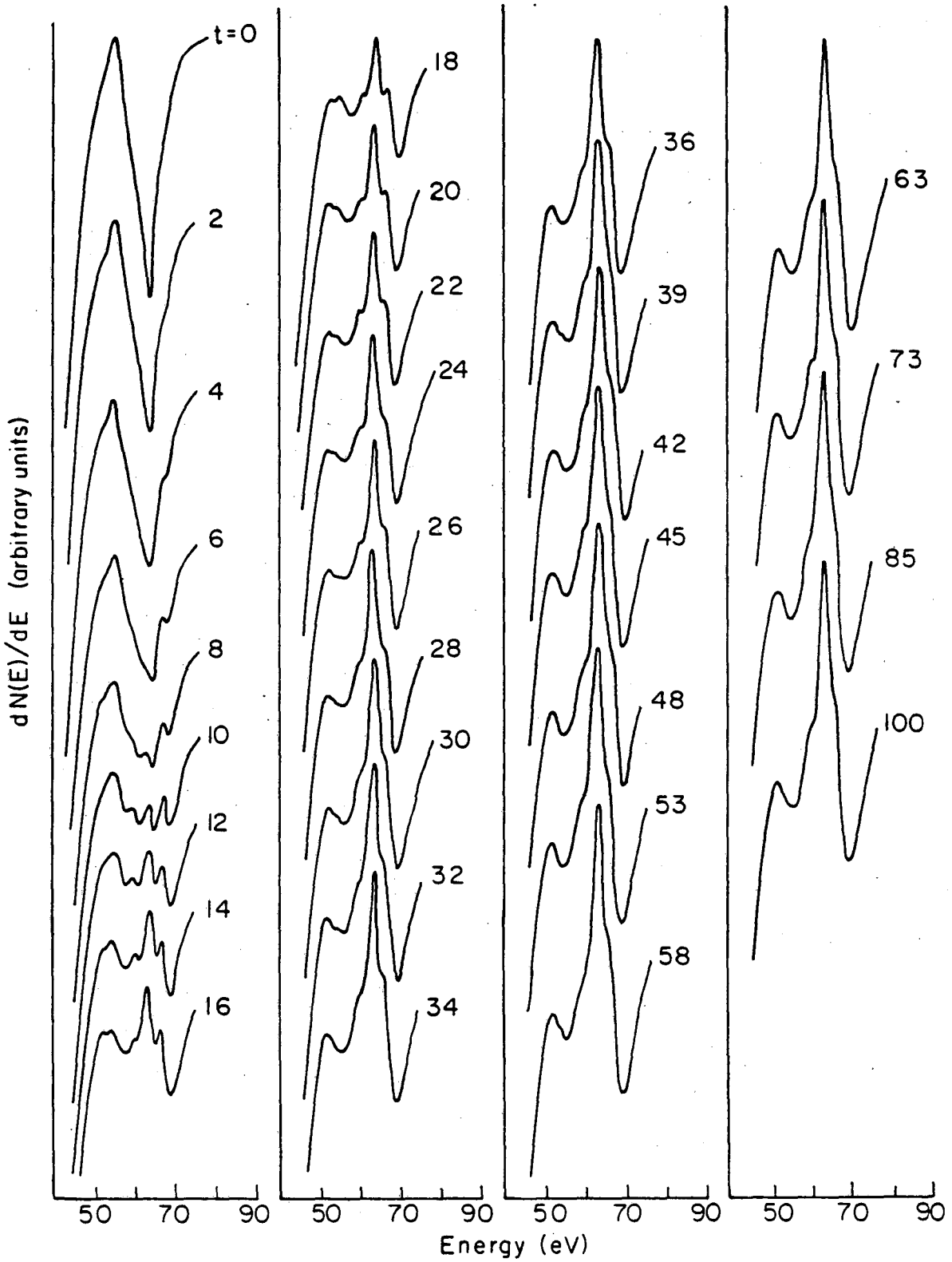
t=0
2
4
6
8
10
12
14
16
18
20
22
24
26
28
30
32
34
36
39
42
45
48
53
58
63
73
85
100
dN(E)/dE (arbitrary units)
50
70
90
Energy (eV)
XBL823-5449

Fig. 1

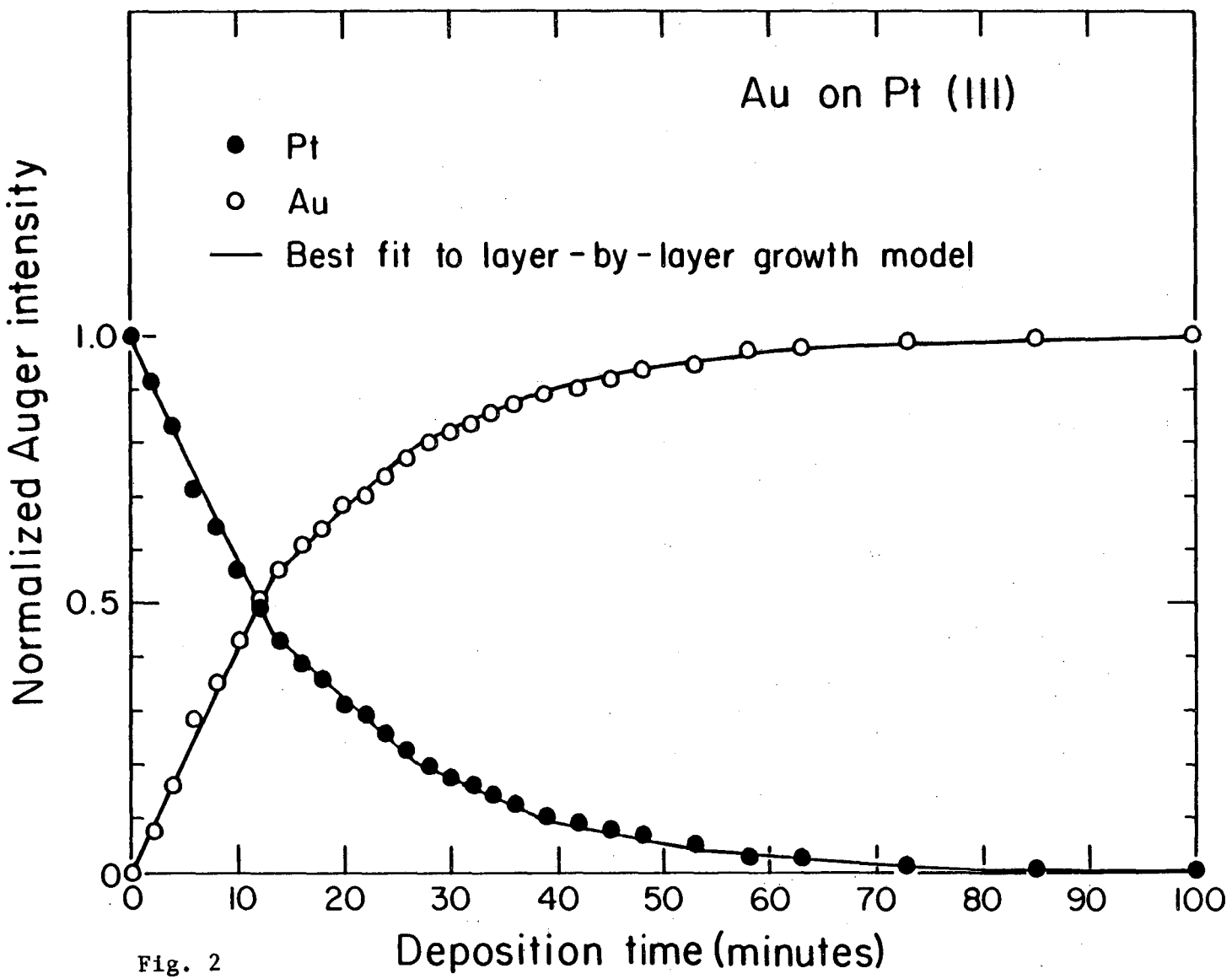

Fig. 2

XBL 819-2489

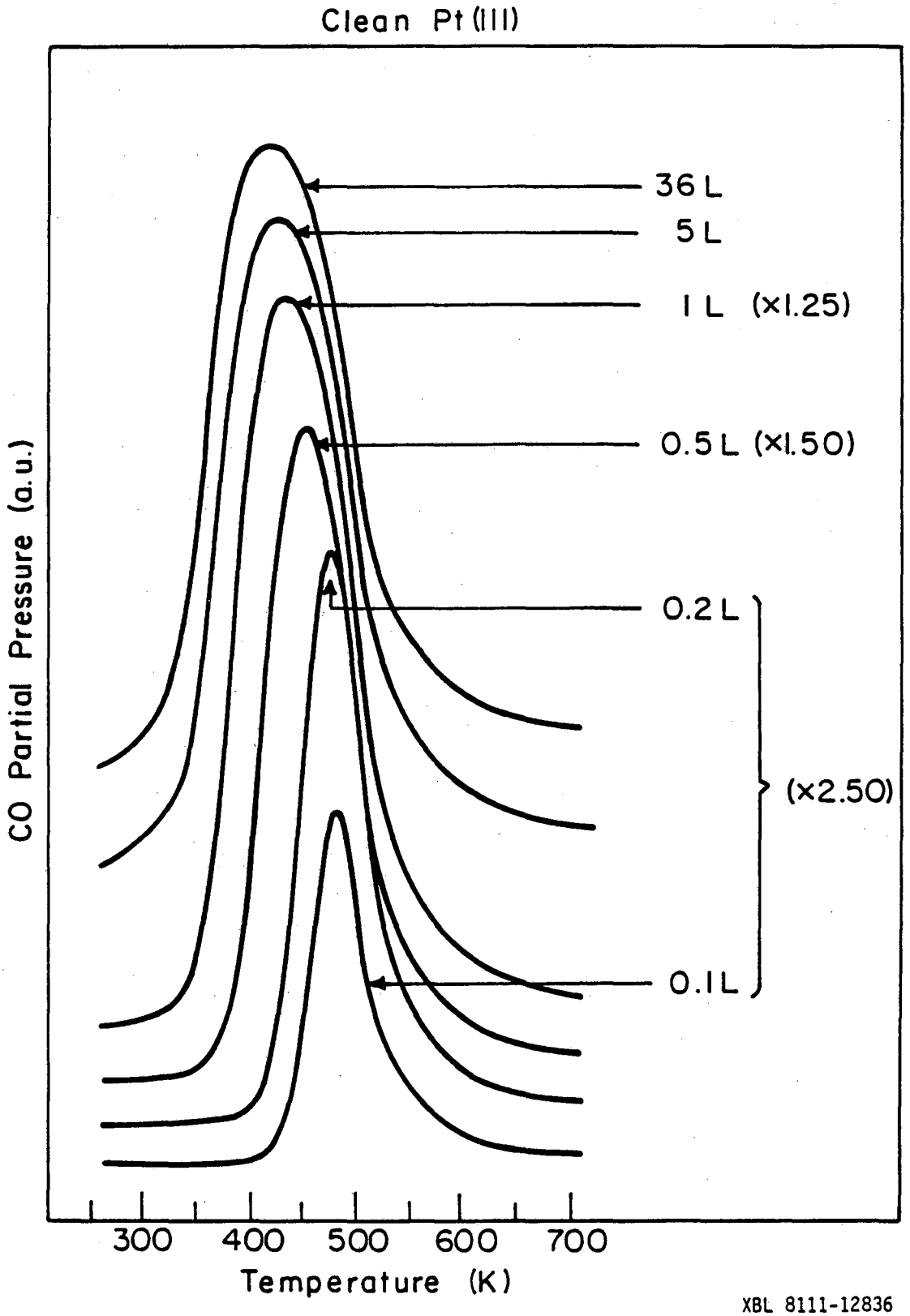

XBL 8111-12836

Fig. 3

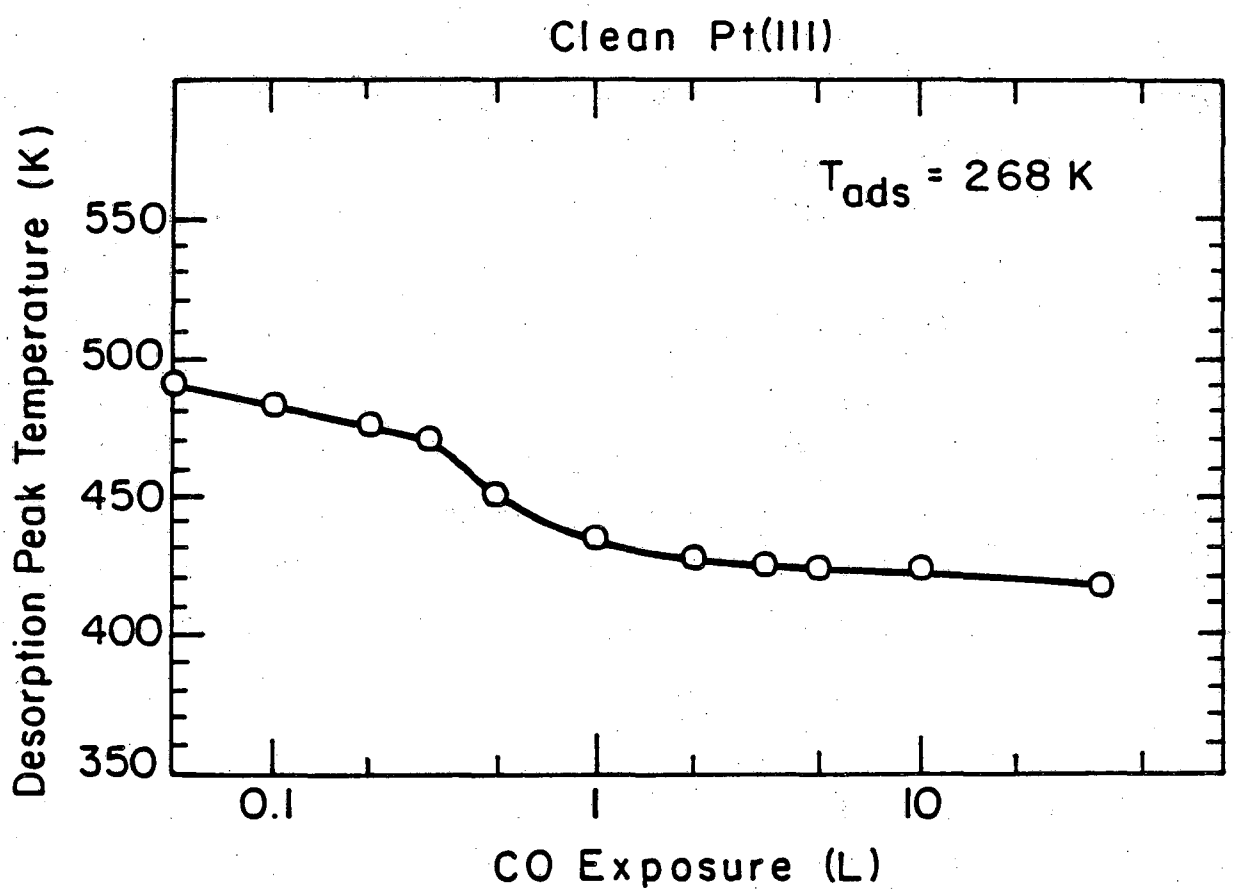

XBL 8111-12835

Fig. 4

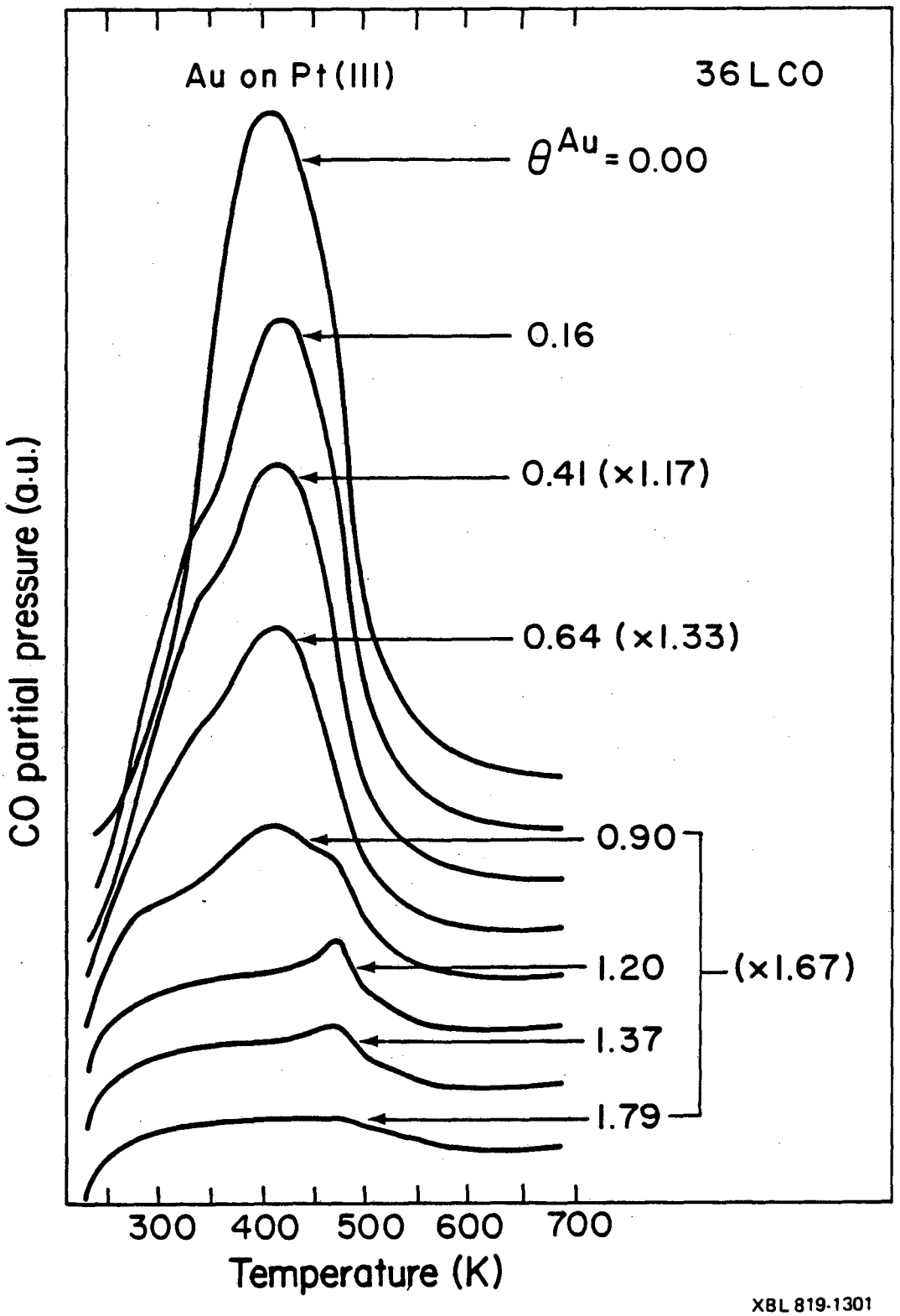
Au on Pt(111)
36 L CO
θ^{Au} = 0.00
0.16
0.41 (×1.17)
0.64 (×1.33)
0.90
1.20
1.37
1.79
(×1.67)
CO partial pressure (a.u.)
300
400
500
600
700
Temperature (K)
XBL 819-1301

Fig. 5

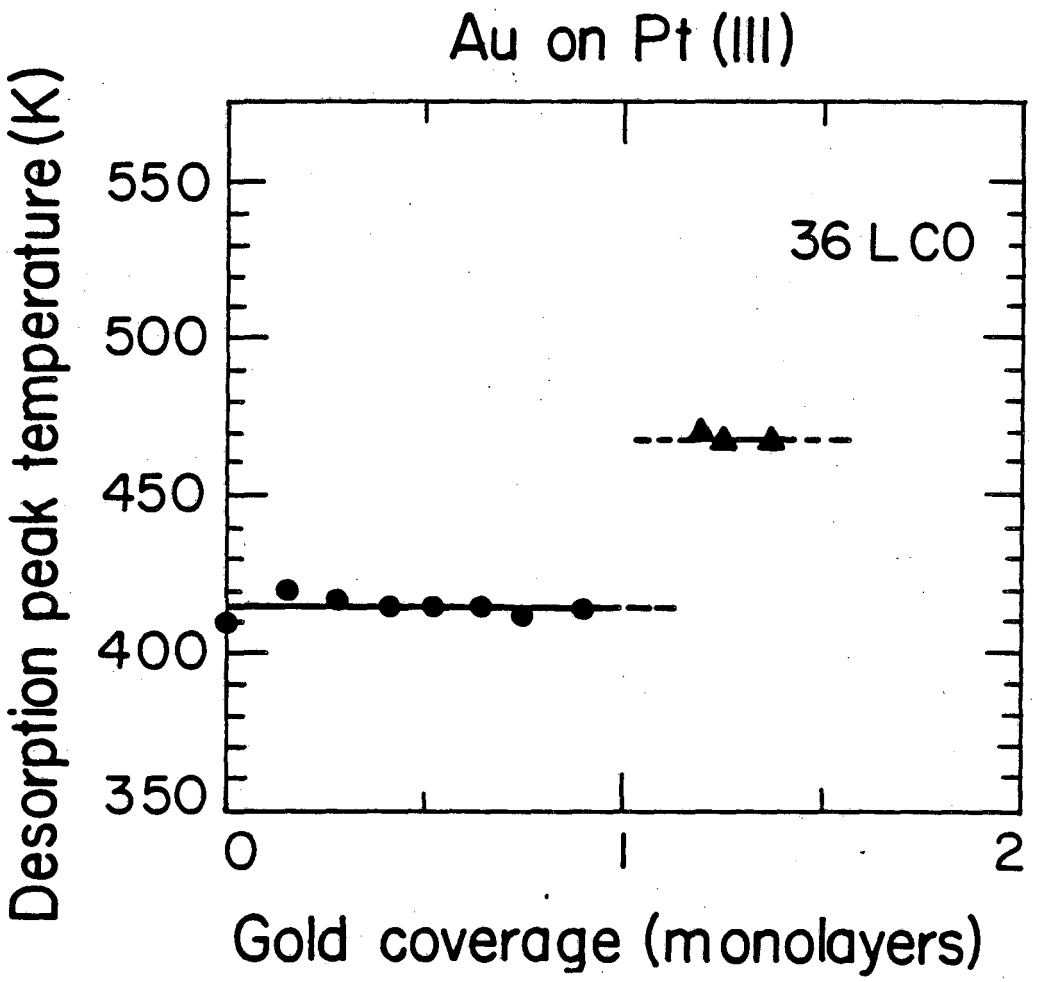

XBL 819-1305

Fig. 6

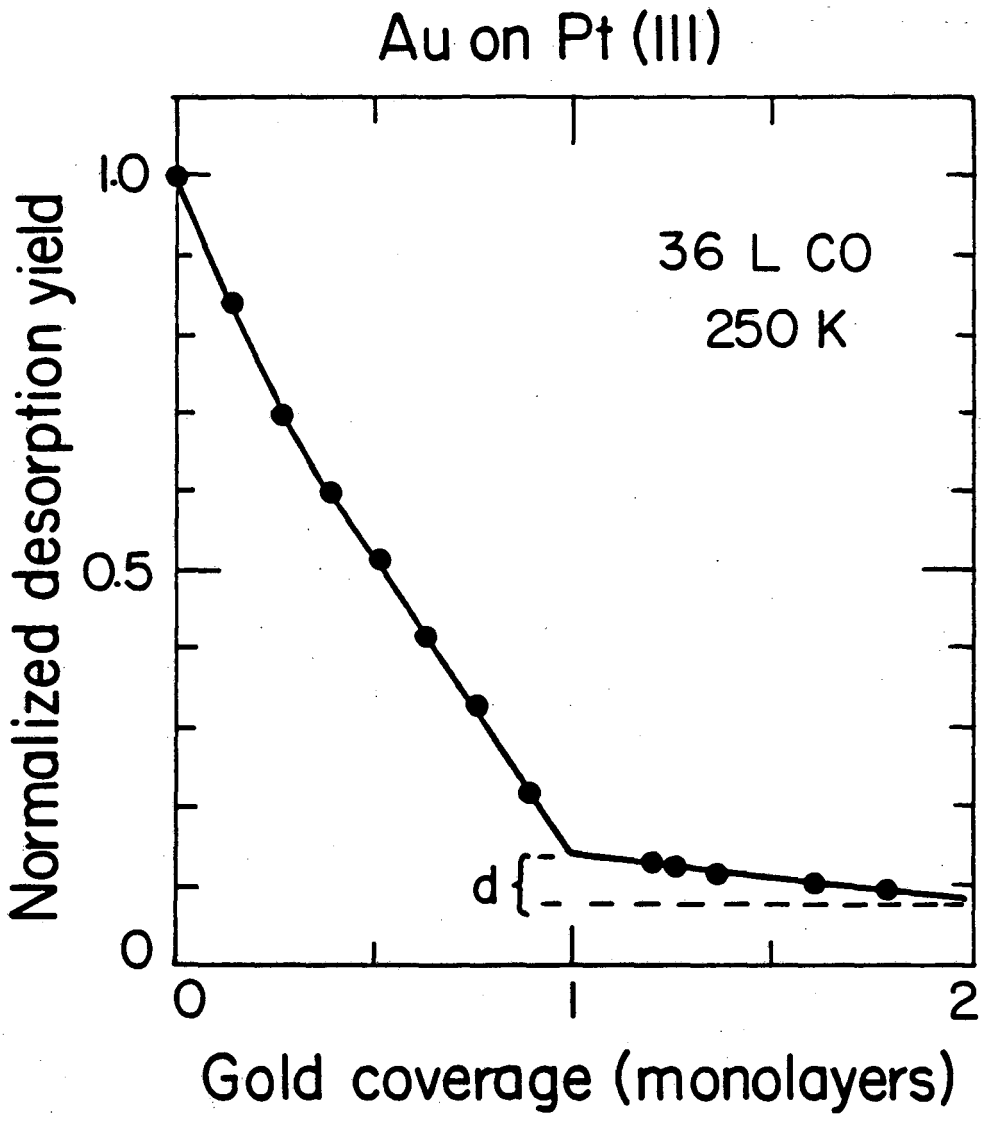

XBL 819-1308

Fig. 7

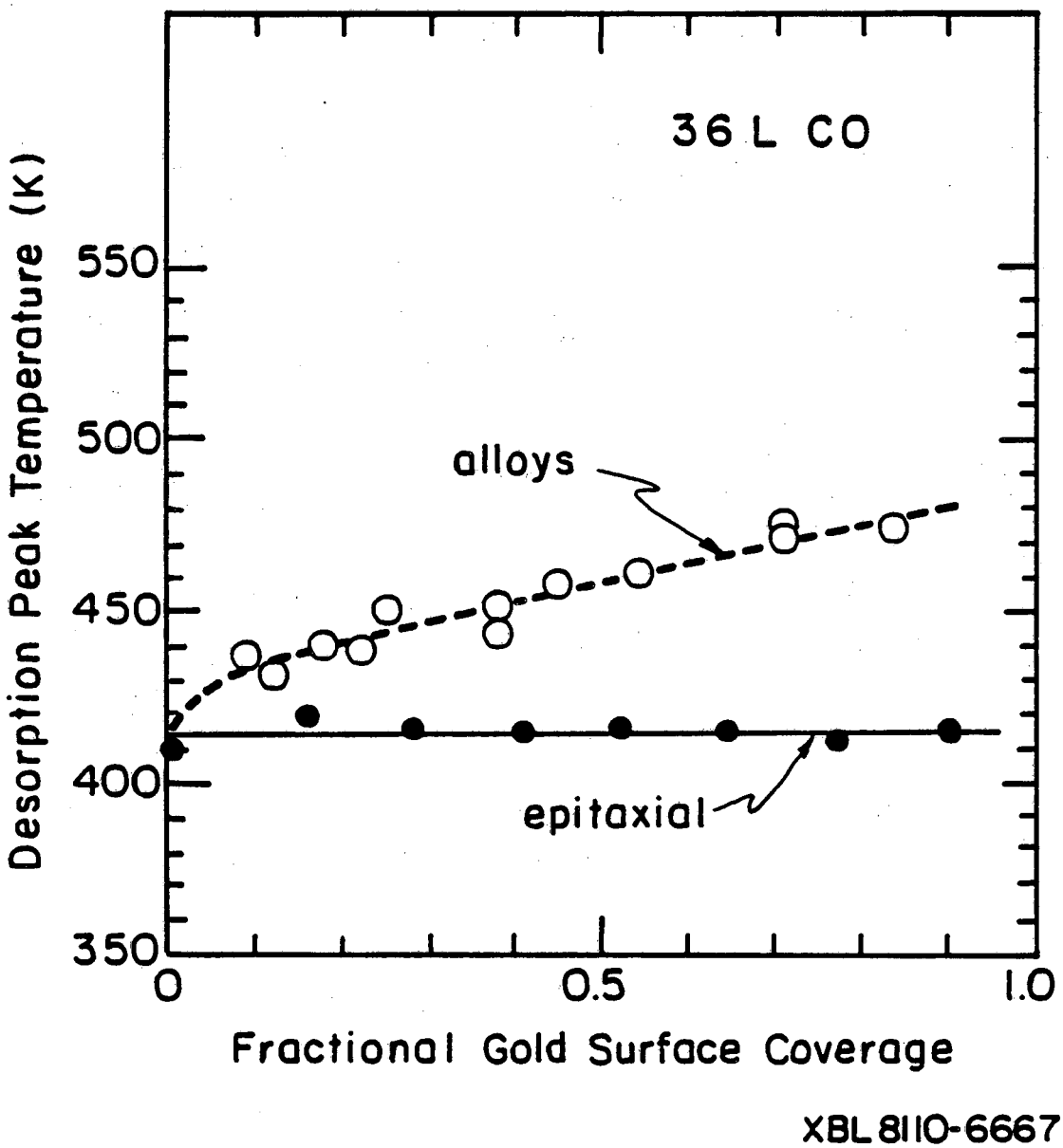
36 L CO
Desorption Peak Temperature (K)
550
500
450
400
350
alloys
epitaxial
0
0.5
1.0
Fractional Gold Surface Coverage
XBL 8110-6667

Fig. 8

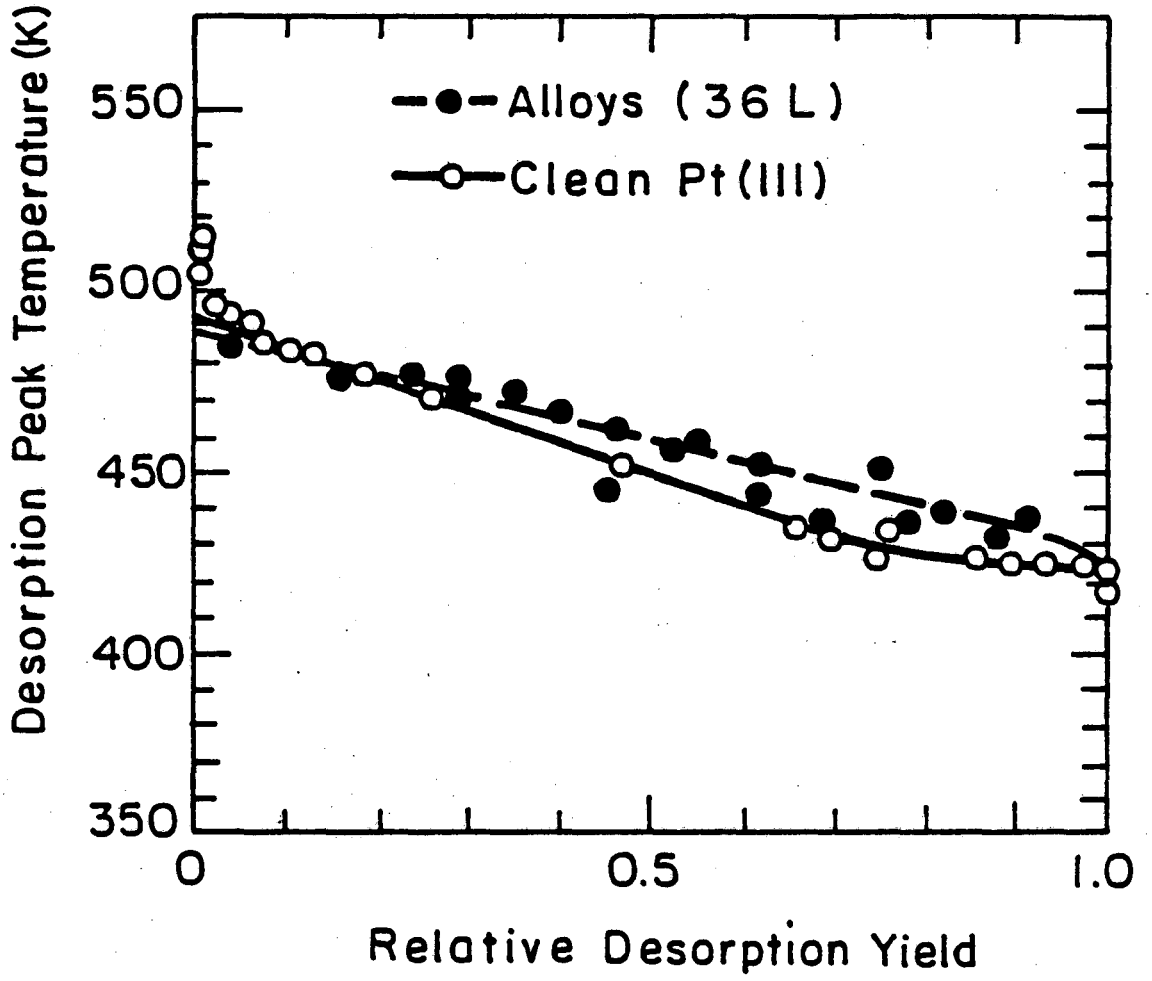

XBL 8111-12834

Fig. 9

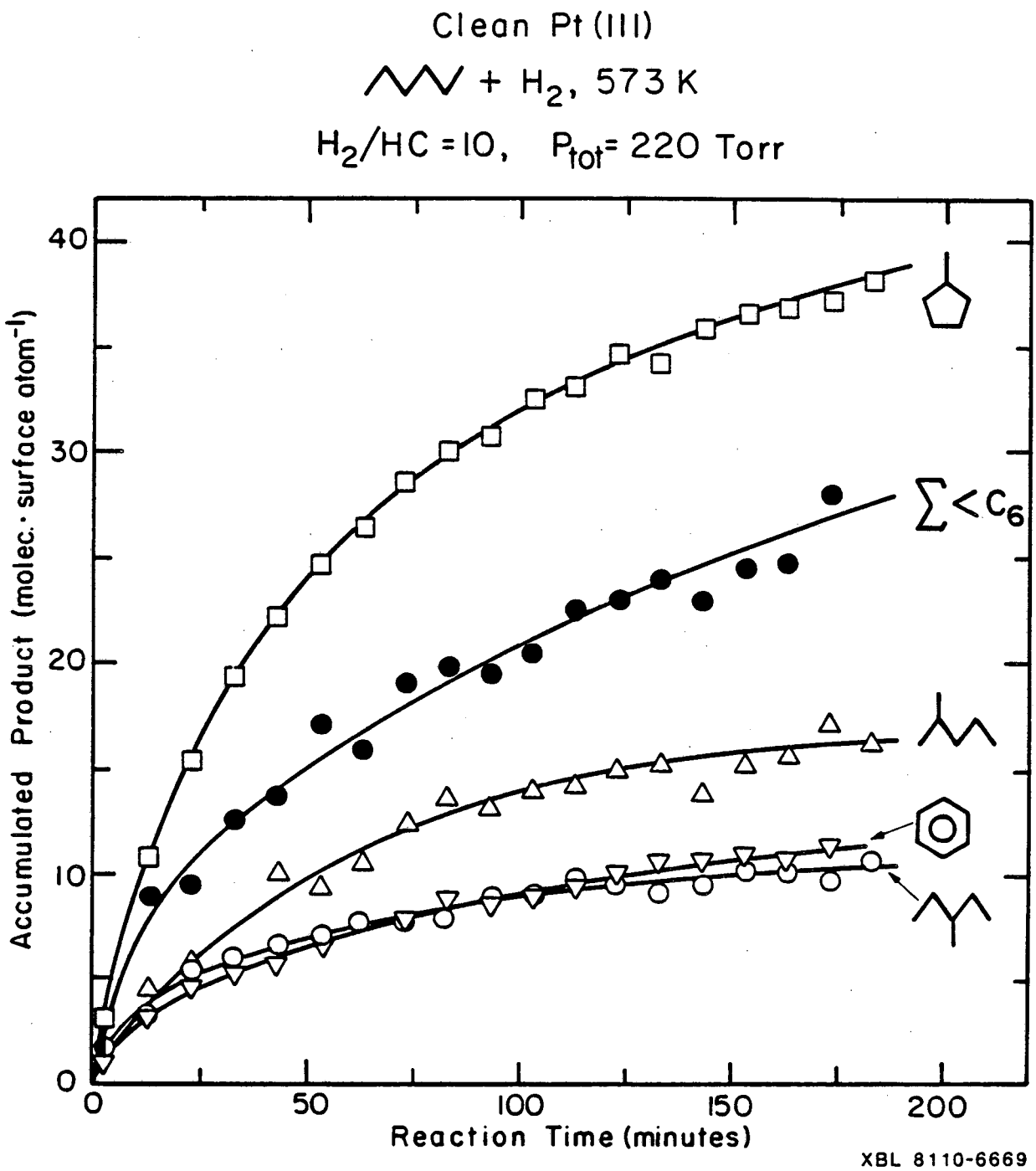
Clean Pt (111)
+ H_2, 573 K
H_2/HC = 10, P_{tot} = 220 Torr
Accumulated Product (molec. · surface atom^{-1})
Reaction Time (minutes)
0
10
20
30
40
50
100
150
200
$\sum < C_6$
XBL 8110-6669

Fig. 10a

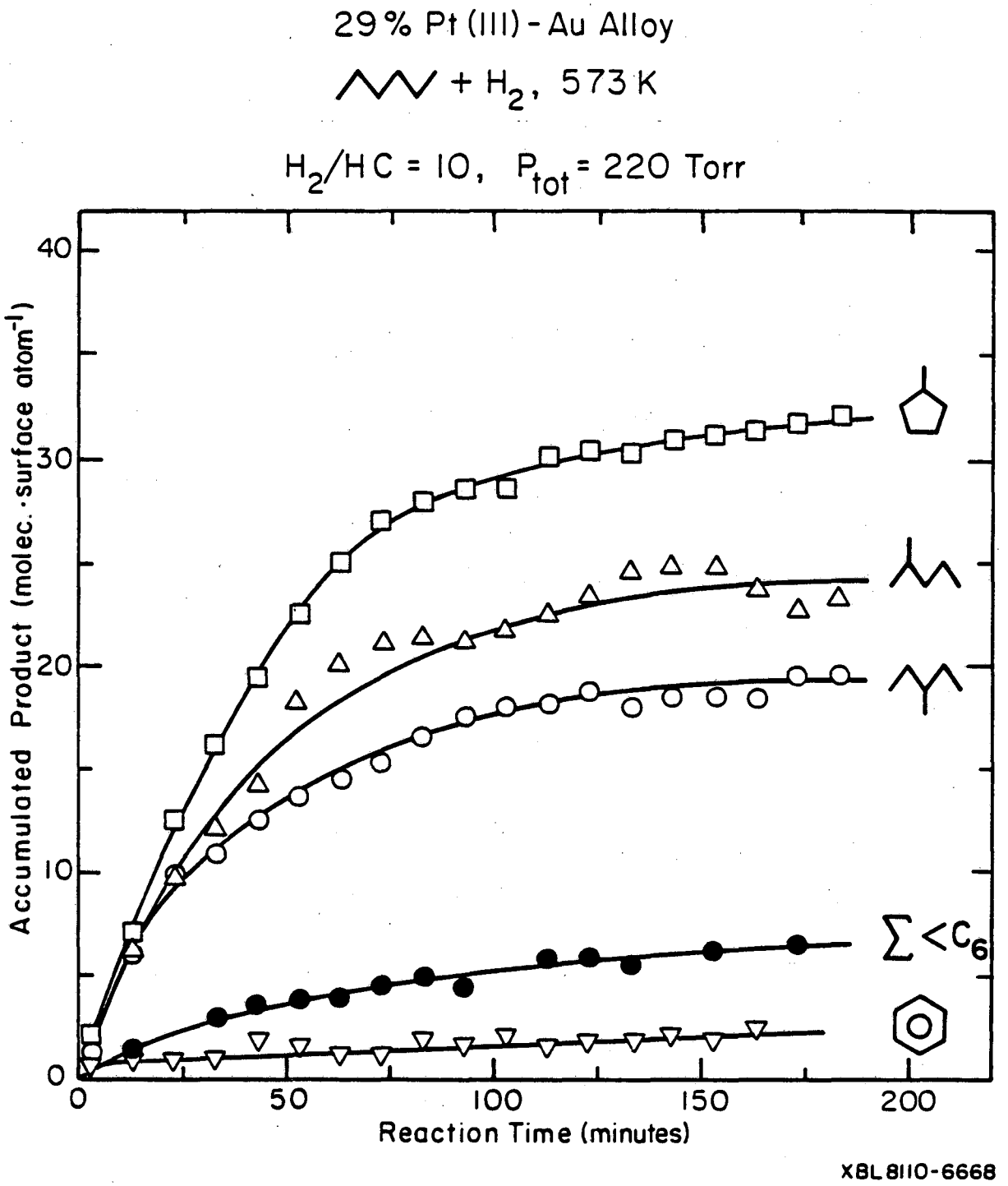
29 % Pt (111) - Au Alloy
+ H2, 573 K
H2/HC = 10, Ptot = 220 Torr
Accumulated Product (molec.·surface atom-1)
Reaction Time (minutes)
0
10
20
30
40
0
50
100
150
200
Σ<C6
XBL 8110-6668

Fig. 10b

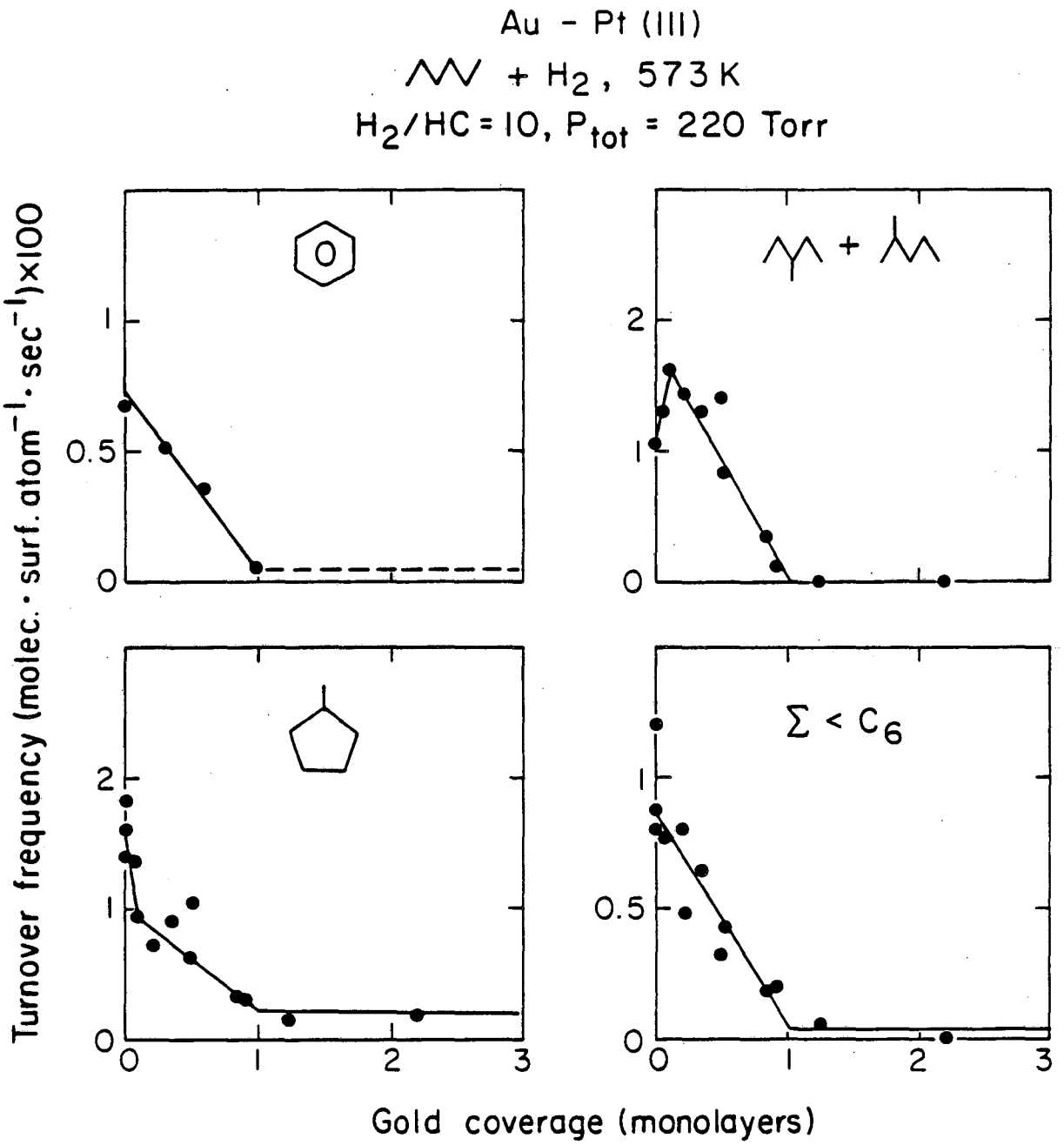

XBL 819-2496

Fig. 11

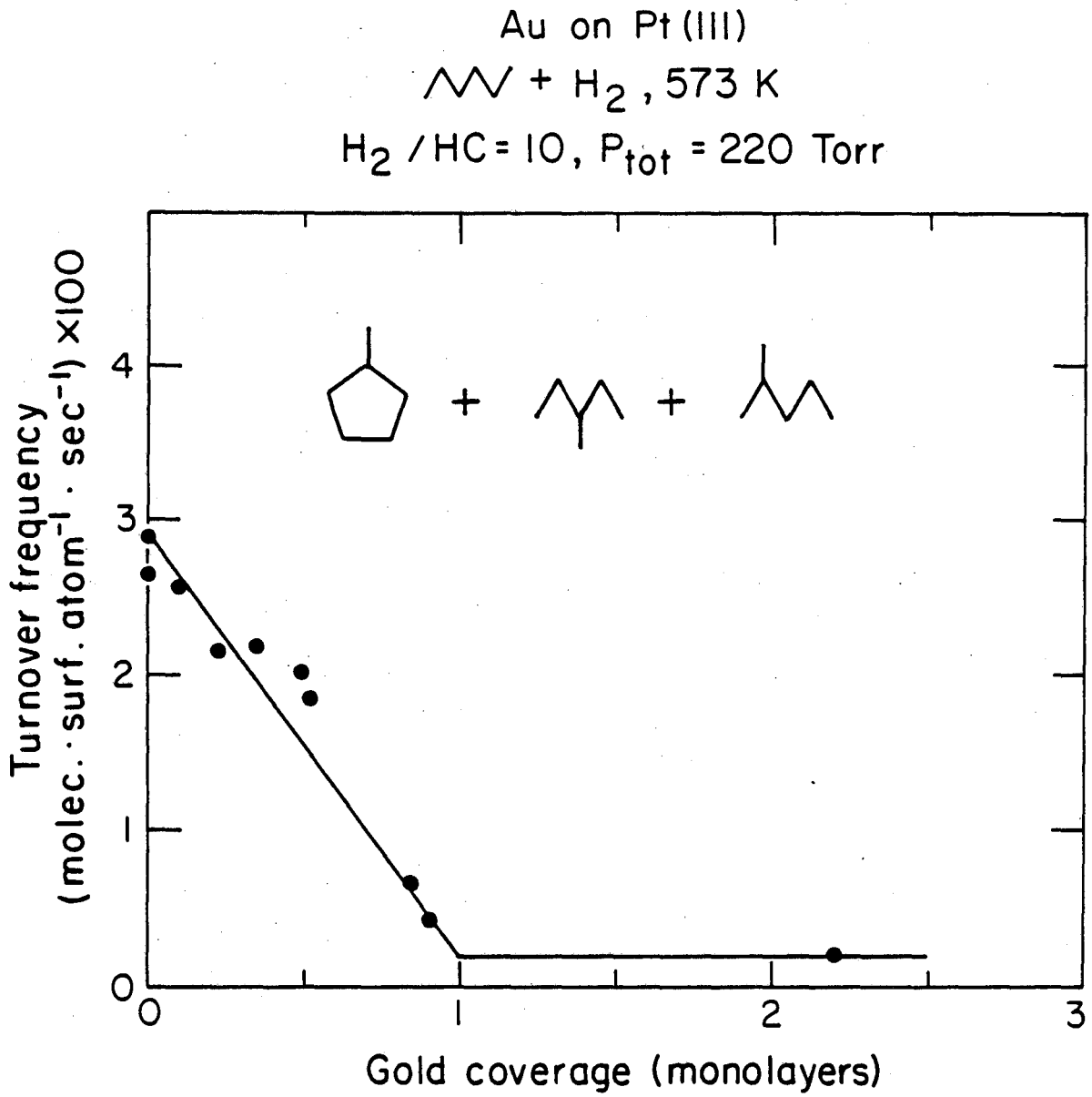

XBL 819-2492

Fig. 12

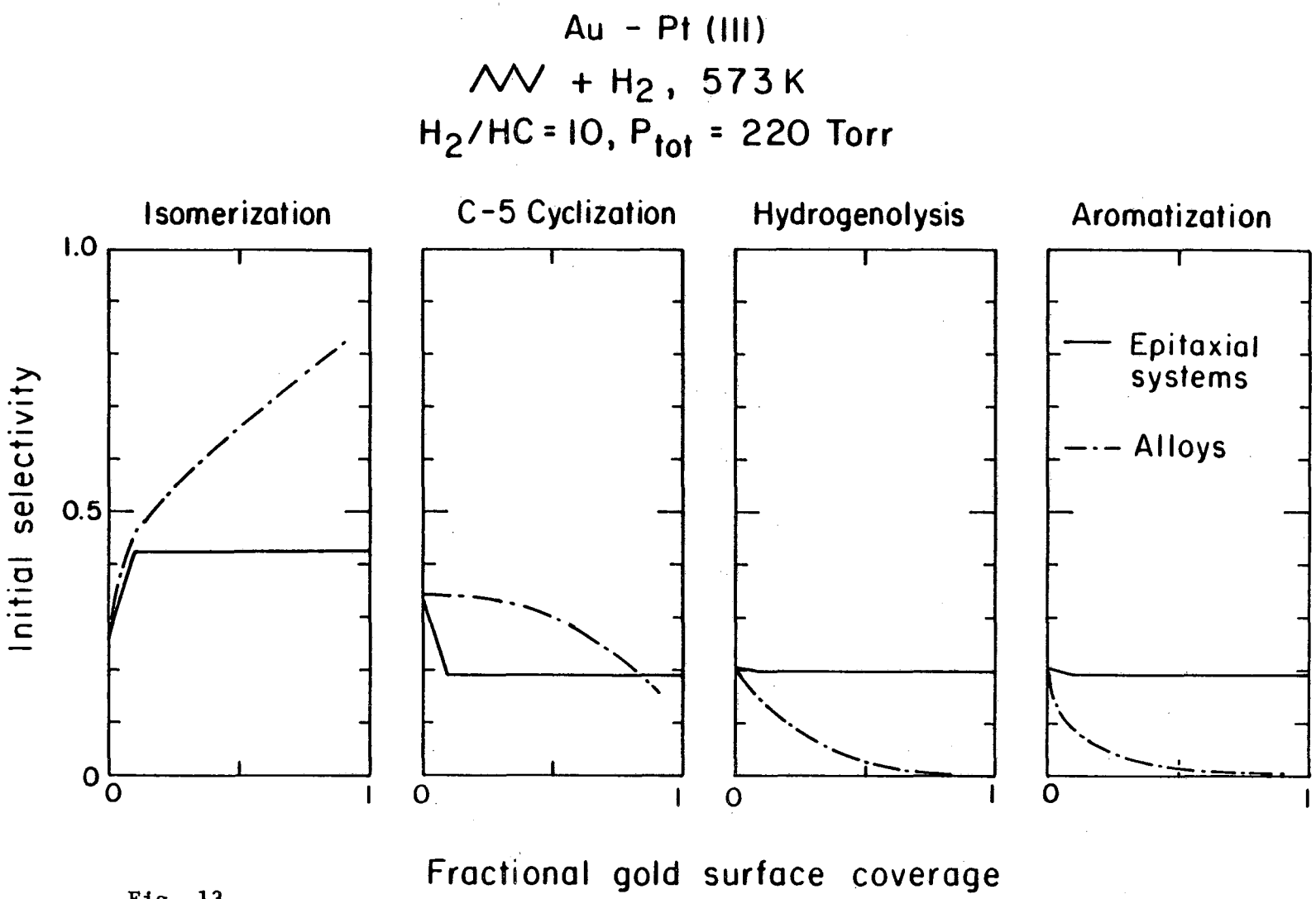

Fig. 13

XBL819-2493

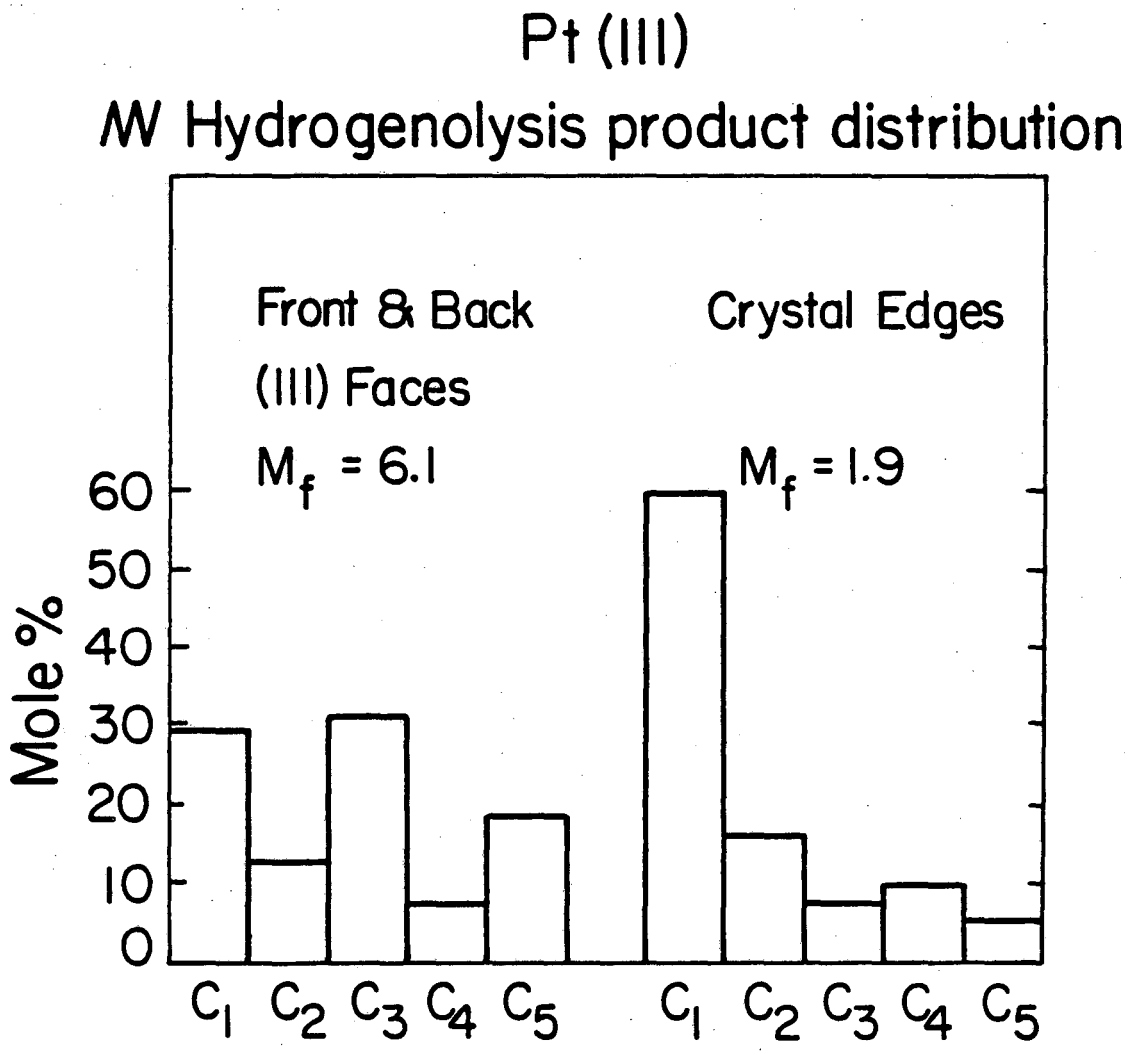

XBL 819-1307

Fig. 14

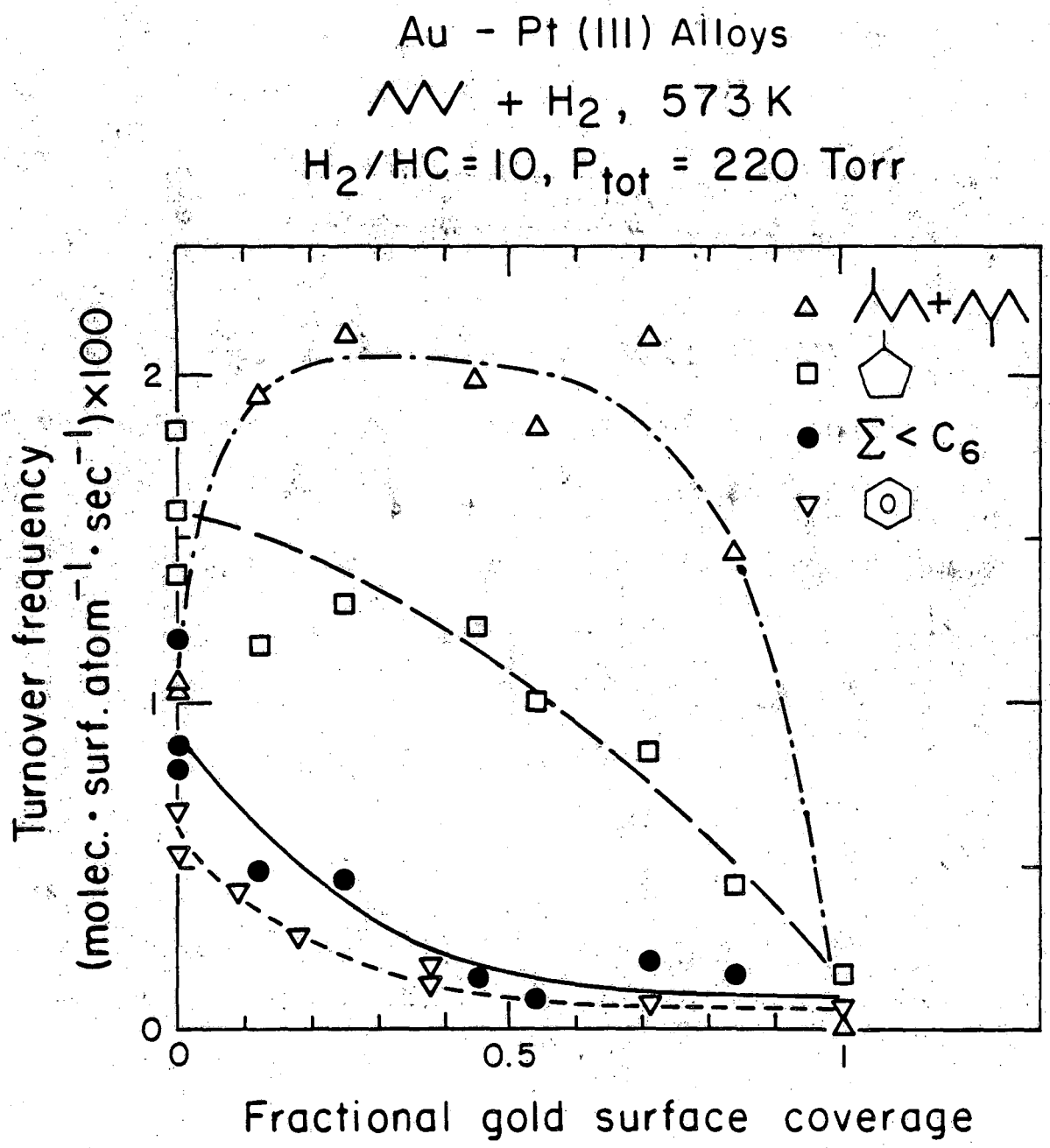

XBL 819-2495

Fig. 15

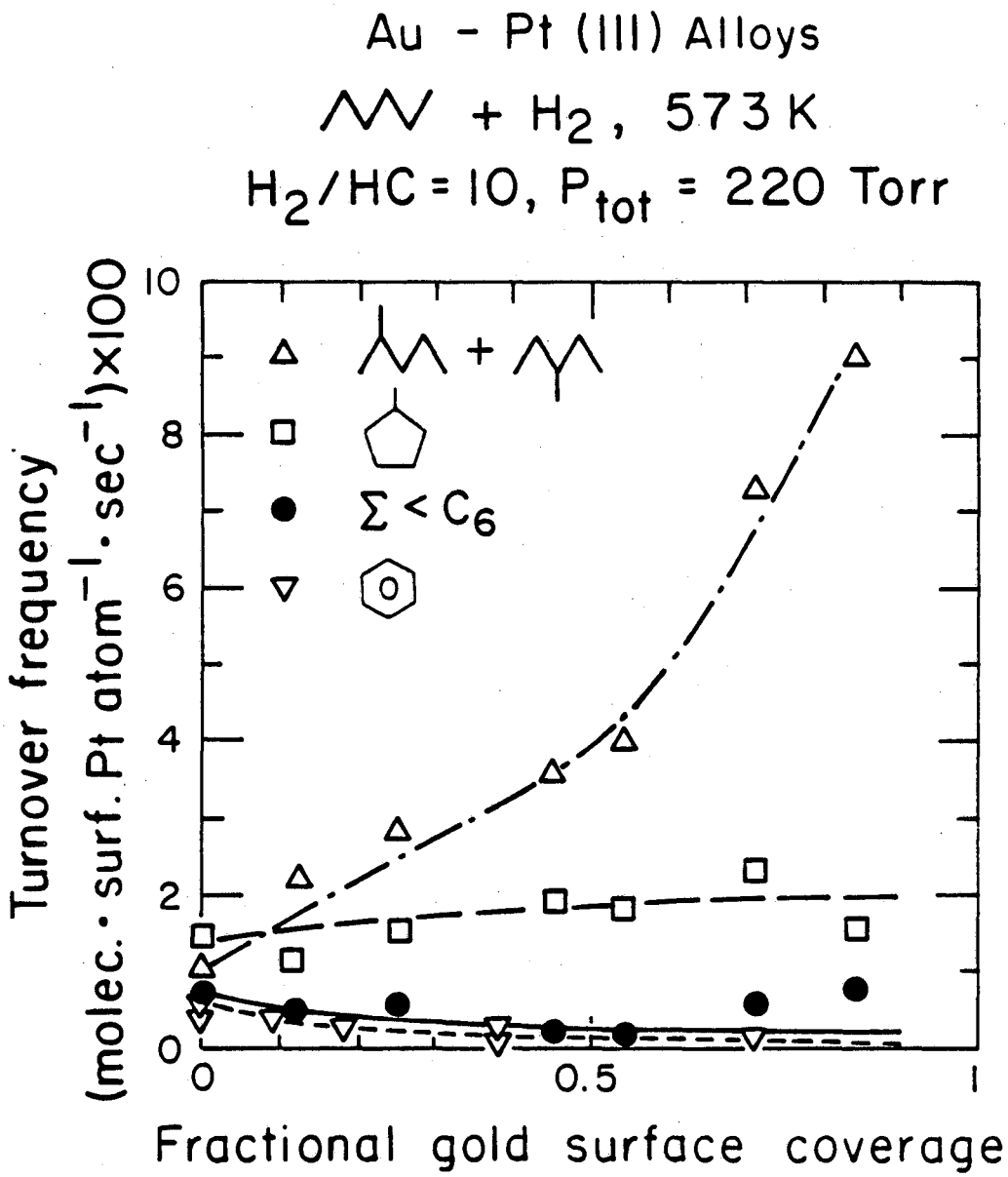

XBL 819-2494

Fig. 16

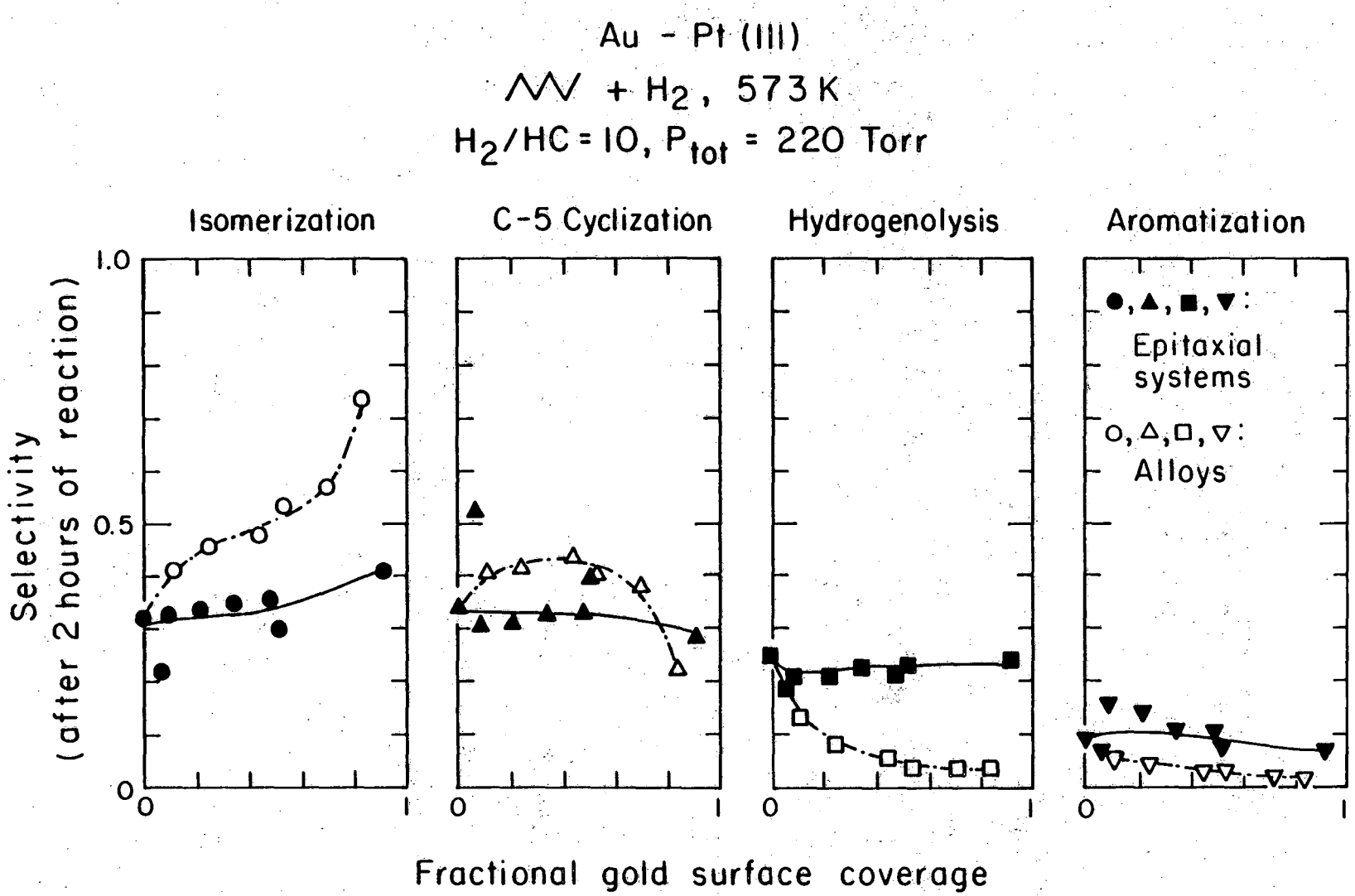

Fig. 17

XBL 819-2490

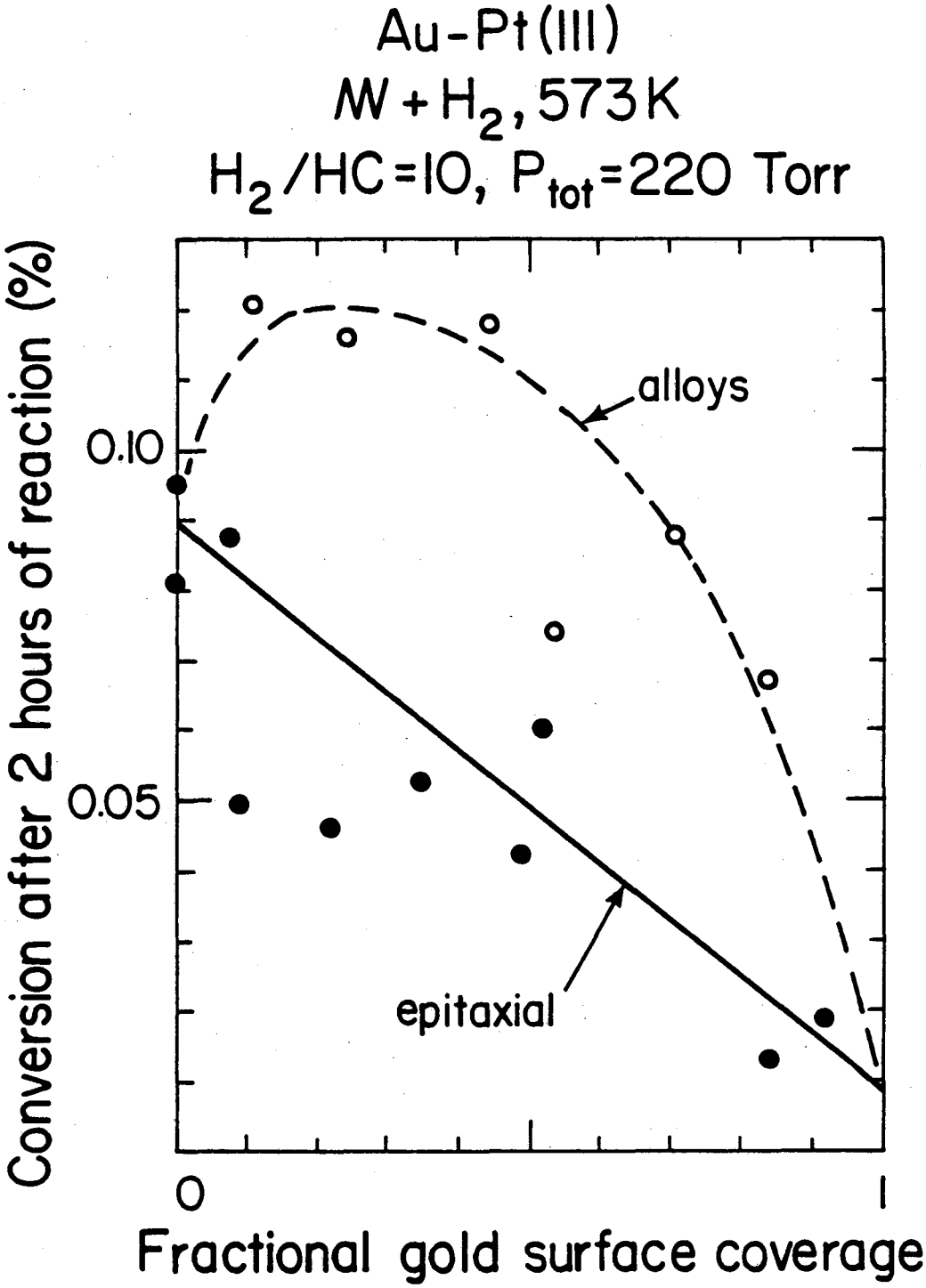

XBL 819-1309

Fig. 18

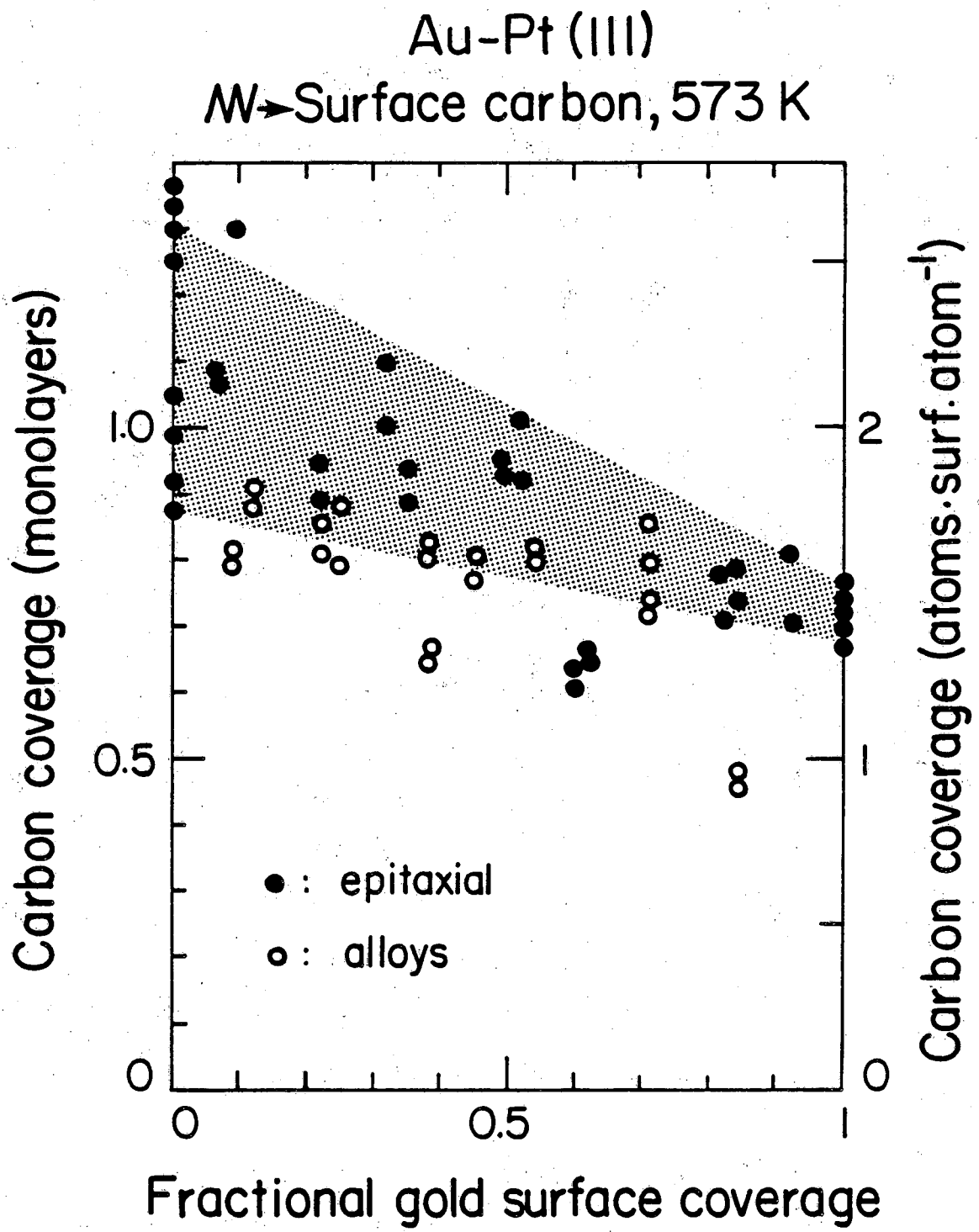

XBL 819-1303

Fig. 19

This report was done with support from the Department of Energy. Any conclusions or opinions expressed in this report represent solely those of the author(s) and not necessarily those of The Regents of the University of California, the Lawrence Berkeley Laboratory or the Department of Energy.

Reference to a company or product name does not imply approval or recommendation of the product by the University of California or the U.S. Department of Energy to the exclusion of others that may be suitable.

TECHNICAL INFORMATION DEPARTMENT
LAWRENCE BERKELEY LABORATORY
UNIVERSITY OF CALIFORNIA
BERKELEY, CALIFORNIA 94720